Resonance or Integration? Self-sustained Dynamics and Excitability of Neural Microcircuits

Raul C. Mureşan[1,2,3], Cristina Savin[1,2,4]

[1]*Frankfurt Institute for Advanced Studies (FIAS), Frankfurt/M, Germany*

[2]*Center for Cognitive and Neural Studies (Coneural), Cluj-Napoca, Romania*

[3]*Max Planck Institute for Brain Research, Frankfurt/M, Germany*

[4]*Technical University of Cluj-Napoca, Faculty of Automation and Computer Science, Cluj-Napoca, Romania*

Running head:

Resonance or Integration? Dynamics of Microcircuits.

Corresponding author:

Dr. Raul C. Mureşan, Frankfurt Institute for Advanced Studies, Max von Laue Strasse 1, 60438 Frankfurt am Main, Germany, E-mail: raulmuresan@yahoo.com

Abstract:

We investigated spontaneous activity and excitability in large networks of artificial spiking neurons. We compared three different spiking neuron models, namely the integrate-and-fire (IF), regular spiking (RS) and resonator (RES). First, we show that different models have different frequency-dependent response properties, yielding large differences in excitability. Then, we investigate the responsiveness of these models to a single afferent inhibitory/excitatory spike, and calibrate the total synaptic drive such that they would exhibit similar peaks of the post-synaptic potentials (PSP). Based on the synaptic calibration, we build large microcircuits of IF, RS and RES neurons and show that the resonance property favors homeostasis and self-sustainability of the network activity. On the other hand, integration is producing instability while it endows the network with other useful properties, such as responsiveness to external inputs. We also investigate other potential sources of stable self-sustained activity and their relation to the membrane properties of neurons. We conclude that resonance and integration at the neuron level might interact in the brain to promote stability as well as flexibility and responsiveness to external input and that membrane properties, in general, are essential for determining the behavior of large networks of neurons.

INTRODUCTION

Neocortical networks of neurons in the brain have two remarkable properties: they can produce activity patterns in the absence of any sensorial input (Arieli et al. 1995) and exhibit vigorous responses when stimulated (Frazor et al. 2004). The internal activity produced by the brain independently of external stimulation is present even during sleep cycles (Evarts 1964; Steriade 2006) or during sensory deprivation (Dupont et al. 2003; Celikel et al. 2004). It has been suggested that self-sustained activity contributes to higher cognitive processes, such as working memory, decision-making and goal-directed behavior (Wang 2003) and it has been recently shown that spontaneous brain activity plays an important role in synaptic maturation during development (Gonzalez-Islas and Wenner 2006).

There are two different concepts associated with self-sustained activity: *spontaneous activity* and *persistent activity*. *Spontaneous activity* is related to ongoing dynamics that is not triggered by external events (Arieli et al. 1995) while *persistent activity* is triggered by an external event/stimulus and is maintained in a task relevant manner (Miyashita and Chang 1988). *Persistent activity* is produced on top of already existing *spontaneous activity*. Our main interest in this study was to investigate possible mechanisms underlying *spontaneous activity* in models of spiking microcircuits and their implications on the *responsiveness* to external inputs.

Spontaneous activity and the *responsiveness* to external inputs are very much interrelated. To be able to maintain robust ongoing activity in the absence of stimulation, a neural circuit must possess some homeostatic mechanisms (Turrigiano and Nelson 2004; Davis 2006) that avoid the "dying out" (activity completely ceases after some period of time) or the "explosion" (the network becomes epileptic) of activity. In turn, such regulation mechanisms might impair the responsiveness of the circuit to external stimuli. This issue becomes critical if the circuit receives

weak inputs and must amplify them to attain a robust response. Indeed, recent evidence suggests that thalamic inputs to the cortex are quite weak. They represent less than 10% of the total number of afferent connections in layer IV (Douglas and Martin 2004). Nevertheless, cortical networks are very responsive to inputs (Frazor et al. 2004) and they exhibit stable *spontaneous activity* that is interacting with input sensory signals to produce a combined effect (Arieli et al. 1996; Arieli 2004; Tsodyks et al. 1999). We suggest that stable *spontaneous activity* and responsiveness to inputs might be supported by very different mechanisms and that there might be a complex interplay between the two.

Spontaneous activity

There have been numerous attempts to model self-sustained activity in artificial spiking neural networks. While *persistent activity* relies on specific neuronal circuitry (Durstewitz and Seamans 2006), *spontaneous activity* is usually modeled using an external, non-specific, "background" input (van Vreeswijk and Sompolinsky 1996; Latham et al. 2000; Plesser and Gerstner 2000; Hansel and Mato 2001; Roxin et al. 2004). The background input is unrelated to the stimulus and is thought to arise mostly from distant cortical or subcortical structures (Amit and Brunel 1997; Durstewitz and Seamans 2006).

A background input is necessary for producing *spontaneous activity*, because stable networks of integrator neurons have a tendency to become quiescent without external excitation (Hansel and Mato 2001). The background input can be modeled either deterministically (van Vreeswijk and Sompolinsky 1996) or stochastically (Brunel and Hakim 1999; Latham et al. 2000; Plesser and Gerstner 2000; Hansel and Mato 2001; Roxin et al. 2004). The vast majority of models use the stochastic approach. A random, usually Poisson process is used in such cases to account for the external background drive that allows the network to maintain a baseline activity level and

avoid “dying out”. Such a strategy has also been motivated by the known spontaneous, apparently random spiking of cortical neurons that would, at least in part, be induced by the random background fluctuations (Tuckwell 1989; Softky and Koch 1993). Indeed, there is increasing evidence that spontaneous neurotransmitter (spike independent) axonal release induces miniature synaptic potentials (minis) that play an important role in promoting spontaneous network activity during sleep and anaesthetized states (Paré et al. 1997, 1998; Timofeev et al. 2000). However, in the awake state, the common belief that neurons fire in a stochastic, unreliable way has been recently challenged (Gur and Snodderly 2006), thus the influence of the random background is probably differentially expressed depending on the cortical state.

It is very likely that in the cortex many mechanisms contribute to the establishment of stable *spontaneous activity*. Spontaneous miniature synaptic events and non-cortical sources of excitation provide a “lower bound” for cortical activity, preventing it from “dying out”. On the other hand, the neocortical circuitry is highly recurrent, hence the danger of self-amplified “runaway excitation” leading to the “explosion” of activity (Vogels et al. 2005). This raises the need for an “upper bound” on neural activity (Davis 2006). The dynamic regulation of network activity is supported by numerous homeostatic mechanisms, such as spike-timing dependent plasticity (STDP) with hard or soft bounds (Abbott and Nelson 2000), short-term synaptic facilitation/depression (Abbott and Regehr 2004), synaptic scaling (Turrigiano and Nelson 2004), intrinsic neuronal plasticity (Zhang and Linden 2003) or spike-frequency adaptation (Benda and Herz 2003; Gabbiani and Krapp 2006). Among these, intrinsic plasticity and synaptic scaling are slow, compared to the response timescale of cortical networks (tens of milliseconds). Synaptic facilitation/depression and STDP can be relatively fast and act at the level of synapses. At the cellular level, spike-frequency adaptation is a fast process that could help networks avoid firing saturation (Gabbiani and Krapp 2006). To the best of our knowledge, in the context of

spontaneous activity, no fast homeostatic mechanism relying on intrinsic membrane properties has been put forward so far. Here, we propose membrane resonance as a possible candidate.

Responsiveness to inputs

It is generally recognized that fast homeostatic processes supporting the stability of network activity also impair its responsiveness to external stimuli (Vogels et al. 2005). Slower regulating mechanisms such as intrinsic plasticity and synaptic scaling are not expected to directly interfere with response dynamics on a short time scale. However, fast mechanisms like short-term depression and spike-frequency adaptation can in principle prevent robust excitatory waves from propagating since they reduce the gain in the network (Turringiano and Nelson 2004). Such control mechanisms can dramatically reduce the responsiveness of the circuit to external stimulation. Reconciling stable *spontaneous* dynamics with network responsiveness is still an unresolved issue (see Vogels et al. 2005 for a review).

In cortical networks, the regulation of the "lower bound" of activity is achieved both by integrating "background/external" excitatory signals (minis/non-cortical drive) and through intrinsic dynamical properties of the network, such as reverberating activity. The "higher bound" is regulated through network properties (that stem from a plethora of mechanisms ranging from synaptic to cellular and structural properties) and also through the global modulation of the cortical state. Here, we first study the possibility of regulating both the "lower" and "higher" bounds of activity exclusively through network properties, in the absence of any external drive. Only a few studies reported so far a success in this direction (Kumar et al. 2005; Mureşan et al. 2005) because of the known difficulty of stabilizing the activity of strongly coupled recurrent neural microcircuits (Vogels et al. 2005) for the general case (stable reverberating circuits can be

produced using specialized circuitry; see: Hansel and Mato 2001; Ben-Yishai et al. 1995; Durstewitz and Seamans 2006). We propose next that membrane properties of individual neurons could play a very important role in both *spontaneous activity* and network responsiveness. We explore the properties of different neural models that are commonly used in building large scale networks of spiking neurons. More specifically, the leaky integrate-and-fire model (Dayan and Abbott 2001) and two variants of the Izhikevich (Izhikevich 2003) model (regular-spiking and resonator neurons) are investigated here. The differences in terms of excitability and frequency-dependent response will be emphasized. To bring the different models of neurons to comparable activity regimes, we first calibrate the synaptic strength required to obtain the same post-synaptic-potential (PSP) peak to an incoming spike. Based on such calibrations, we are able to compare large networks of integrate-and-fire, regular-spiking and resonator neurons and investigate their ability to produce stable *spontaneous activity* in the absence of any external drive. We also investigate the responsiveness of such networks to external inputs and we discuss different patterns of activity that are produced by the integrative or resonant behavior of network neurons. We finally investigate the relationship of our findings with other known processes contributing to *spontaneous activity* such as the influence of miniature synaptic potentials and synaptic delays.

METHODS and RESULTS

Integration or resonance?

Since the early studies of Sherrington (Sherrington 1906) it has been mostly believed that neurons behave as integrators. The integrative property of neurons implies that responses of neurons to stimulation increase monotonically with the increasing input frequency.

However, recent experimental evidence suggests that apart from their integrative properties, neurons also exhibit frequency dependent behavior or resonance, having preferred stimulation frequencies in the range of 5-20 Hz for pyramidal neurons and 5-50 Hz for interneurons (Hutcheon and Yarom 2000; Fellous et al. 2001). The resonant property implies that neurons have a maximal response to a preferred stimulation frequency. It has been shown that the original Hodgkin-Huxley model (Hodgkin and Huxley 1952) behaves more like a resonator than an integrator (Izhikevich 2000).

In spite of such evidence, most modeling studies on networks of spiking neurons use the simple leaky integrate-and-fire model (IF). While it is computationally easy to simulate, the model does not exhibit realistic dynamics comparable to cortical neurons (Izhikevich 2004). The IF neuron belongs to class 1 excitable systems and increases its response with the increasing stimulation frequency monotonically. The IF formalism models only one variable, namely the membrane potential *(v)* of neurons (Dayan and Abbott 2001):

$$\tau \frac{dv}{dt} = -v + R \cdot I \qquad (1)$$

where, v – membrane potential, τ – membrane time constant (typically 10 ms), R – membrane resistance (taken here to be 10 MΩ), I – total post-synaptic (input) current.

The Hodgkin-Huxley-type (HH) models fit the dynamics of real neurons better than the linear integrate-and-fire formalism which cannot reproduce the variable threshold behavior of cortical cells. However, the original HH model is computationally demanding, rendering it unfeasible for the study of large networks of neurons (Izhikevich 2004). Recently, a more efficient model has been proposed (Izhikevich 2003). It is based on two-dimensional reduced Hodgkin-Huxley approximations and it is very efficient in terms of computational complexity. The Izhikevich model (Izhikevich 2003) discussed here uses two variables to describe the state of the neuron: the membrane potential *(v)* of the neuron and a recovery variable *(u)*:

$$\frac{dv}{dt} = 0.04v^2 + 5v + 140 - u + I \qquad (2)$$

$$\frac{du}{dt} = a \cdot (bv - u) \qquad (3)$$

where v – membrane potential, u – recovery variable, I – total post-synaptic current, a,b – parameters.

When the membrane potential reaches a value larger than 30 mV, a spike is recorded and the membrane potential is reset to its resting value, while the recovery variable is increased by a given amount:

$$v = c; \quad u = u + d \qquad (4)$$

where c – resting potential, d – a parameter that is added to the recovery variable.

Depending on the concrete value of the four parameters *(a,b,c,d)*, the model can reproduce a plethora of behaviors of cortical neurons, like adaptation, post-inhibitory rebound, etc (Izhikevich, 2003). Of special interest to our study is the regular spiking (RS) regime *(a = 0.02, b = 0.1, c = -70 mV, d = 8)* and the resonator (RES) regime *(a = 0.1, b = 0.26, c = -70 mV, d = 2)*. While in the regular spiking regime the neuron is behaving intermediately between an integrator and a resonator, exhibiting spike-frequency adaptation, in the resonator regime the membrane

potential tends to oscillate after stimulation and the neuron can be switched between silent and spiking modes by appropriately timed stimuli (Izhikevich 2002).

We model the total input current *(I)* that a neuron receives as the sum of all post-synaptic currents *(psc_i)* produced at each synapse *i*:

$$psc_i = A_{syn} \cdot W_{syn} \cdot g \cdot (E_{syn} - v_{post}) \quad (5)$$

$$\frac{dg}{dt} = -\frac{g}{\tau_{syn}} \quad (6)$$

where, psc_i – post-synaptic current contributed by synapse *i*, A_{syn} – an amplitude parameter that determines the maximal amplitude of the *psc*, W_{syn} – the synaptic strength $(W_{syn} \in [0..1])$, *g* – the instantaneous synaptic conductance, E_{syn} – the reversal potential of the synapse (taken 0 mV for excitatory synapses and -90 mV for inhibitory synapses), v_{post} – the membrane potential of the post-synaptic neuron, τ_{syn} – the time constant for the decay of the synaptic conductance after the neurotransmitter release (typically 10-15 ms).

In our simulations, for one given network, and one given model of neuron, there is only one synaptic amplitude (A_{syn}) for all excitatory/inhibitory synapses respectively. Only the synaptic weights (W_{syn}) are different, yielding different coupling efficacies for different synapses (see Eq. 5). The synaptic amplitude can be regarded as a scaling factor that allows one to calibrate the range of coupling efficacies in the entire network.

Each time an afferent spike reaches the synapse, the instantaneous conductance is increased by a constant value (here 1):

$$g = g + 1 \quad (7)$$

Throughout this study, most models (except the Izhikevich neuron) have been integrated iteratively, using the Euler method, with a step of 1 ms. To insure numerical stability for the Izhikevich model, the integration step of the membrane potential equation (Eq. 2) is 0.5 ms (see

Izhikevich 2003). The relatively large step for the Euler integration provides a reasonable precision for the particular models studied here and has the advantage of allowing for large networks to be simulated in reasonable time.

We consider next three models of neurons: integrate-and-fire (IF), regular spiking (RS) and resonator (RES). In the first step of our analysis we assessed the frequency-response properties of these three models.

Subthreshold behavior

Biological neurons can exhibit different dynamics depending on the regime in which they operate (Hutcheon and Yarom 2000). In subthreshold conditions, many neurons display marked resonant properties, i.e. have preferred input frequencies to which they respond maximally. A common technique for characterizing subthreshold behavior is to stimulate the neuron with a subthreshold sinusoidal current having gradually increasing frequency (also called ZAP function) and computing the frequency-dependent impedance of the neuron (Puil et al. 1986). We used here the following subthreshold input stimulus:

$$I(t) = 0.2 \cdot \sin(\alpha \cdot t^{\beta}) \qquad (8)$$

where *I(t)* – the time varying input current injected into the neuron, α – a constant used to scale the frequencies (taken to be $2*PI*10^{-7}$), β – the exponent that determines how fast the frequency increases (chosen with a value of *3* here).

The frequency-dependent impedance *Z(f)* in the subthreshold regime can be computed by dividing the frequency spectra of the responses (membrane potential fluctuations around the resting potential) by the frequency spectrum of the input current, for each frequency component *f* (Puil et al. 1986):

$$Z(f) = \frac{FFT\ of\ voltage\ response(f)}{FFT\ of\ input\ current(f)} \quad (9)$$

where, *Z(f)* – the input impedance of the neuron for subthreshold stimulation with frequency *f*, *FFT(f)* – denotes the Fast Fourier Transform value for the frequency component *f*.

We have stimulated IF, RS and RES neurons with an input ZAP current lasting for 1024 ms (a duration that facilitates easy computing of FFT, our sampling bin size being 1 ms) and computed the frequency spectra of the membrane potential deviations from rest for the three types of neurons (FIG. 1). For each neuron type, we next determined the frequency dependent impedance by dividing the spectra of the membrane potentials by the spectrum of the input current, and taking the complex amplitude as a value for the impedance (Puil et al. 1986).

The membrane potential response and impedance reveal a passive behavior for the IF neuron, just like expected for the case of an RC electrical circuit (Hutcheon and Yarom 2000). Remarkably different, the RS neuron's impedance has a very broadly tuned peak at about 40 Hz, remaining rather unselective for all frequencies. Its impedance is low compared to the other neurons. The RES neuron is a clear resonator, acting as a band pass filter (Hutcheon and Yarom 2000). It is well tuned to a central frequency of 52 Hz and has cutoff frequencies of ~25 Hz and ~84 Hz (see FIG. 1).

Insert FIG. 1. about here.

Suprathreshold behavior

The subthreshold behavior is not guaranteed to be maintained in suprathreshold regimes (Hutcheon and Yarom 2000). Since the interesting regime is when neurons are often crossing the threshold and fire action potentials, it is very important to study how they respond with output spikes to input spike trains.

To determine the suprathreshold behavior of IF, RS and RES neurons we have considered a simple experiment: one neuron of each type was stimulated with input spike trains having various frequencies. The input spike trains had been generated using a homogenous Poisson process with a fixed rate (the input frequency) yielding an exponential distribution of the inter-spike intervals (ISI) (Softky and Koch 1993). The Poisson model for the input spike train has been chosen for simplicity, since the same results would be obtained with a perfectly regular spike train having the same firing rate. However, in the latter case, the response function is not as smooth as in the former case. Using a Poisson input enables the averaging over multiple trials and hence a smoother approximation of the response function (for the perfectly regular case, averaging is irrelevant since there is no variability in the input).

Input frequencies were varied from 5 to 100 Hz in steps of 5 Hz. For each frequency of interest, a Poisson input spike train was produced, in a window with a length inversely proportional to the frequency (see FIG. 2). The window size was increased for low frequencies, such that, on average, a model neuron received roughly equal number of input spikes for all frequencies. In addition, we varied the strength of the synapse that delivered the post-synaptic current to the model neurons.

Insert FIG. 2. about here.

We monitored the total number of postsynaptic spikes induced by the input spike-trains for various input synapse amplitudes. For each input frequency f and each synaptic amplitude A_{syn}, the response of the model neurons $\Psi(f,A_{syn})$ was computed as an average of the total number of postsynaptic spikes over 200 trials (each trial with a different instantiation of the input spike train).

$$\Psi(f, A_{syn}) = \frac{\sum_{i=1}^{N_t} N_s(i)}{N_t} \qquad (10)$$

where, Ψ – the response of a model neuron, f – the frequency of the Poisson input spike train, A_{syn} – the amplitude of the afferent synapse used to stimulate the model neuron, N_t – the number of trials (200 in our case), $N_s(i)$ – the number of postsynaptic spikes in trial i.

In addition to the response function Ψ, we computed the firing rate R of the model neurons by dividing the response function by the length of each window W_s corresponding to each frequency f, as indicated in FIG. 2, right.

$$R(f, A_{syn}) = \frac{\Psi(f, A_{syn})}{W_s(f)} \tag{11}$$

Results in FIG. 3 show very different behaviors of the three models. The integrate-and-fire model behaves as expected, increasing its response with the increasing input frequency monotonically. The higher the stimulation frequency, the higher the response of the IF neuron is (FIG. 3, top-left).

The regular spiking and resonant neurons behave quite differently. The first observation is that their response is non-linear and non-monotonic. Both RS and RES models exhibit two different regimes of activity that depend on the coupling strength (synaptic amplitude). For weak coupling, the responses are increased for frequencies between 25-60 Hz, indicating resonance phenomena (FIG. 3, middle-left and bottom-left). Resonance is more pronounced in the case of the RES model (FIG. 3, bottom-left). For intermediate coupling, both models show an abrupt transition (indicated by arrows in FIG. 3, left), more pronounced for RES neurons, shifting the preferred frequency to very low frequencies while high frequencies are heavily dampened. In this second activity regime, that holds for strong coupling as well, neurons tend to get less and less responsive as the input frequency is increased. At a closer inspection, the response landscapes of the two models are quantitatively different. The most prominent feature of the RES model is its relatively good response even for weak coupling and its more saturated regime for strong

coupling. These features will become important for network homeostasis, as we shall discuss later.

Insert FIG. 3. about here.

We have to mention that the response function Ψ depicted in the left part of FIG. 3 is isolating the frequency response component for suprathreshold stimulation. However, this doesn't mean that the firing rate of RS and RES neurons is not increasing for higher stimulation frequencies. The firing rate R of model neurons, shown in FIG. 3 right, reveals more qualitative differences between models. Although all neurons tend to increase their firing rate for higher input frequencies, the RS and RES neurons have a more moderate slope for the increase. Moreover, the RES neuron exhibits vigorous responses even for weak coupling, while its firing rate has a tendency to saturate for high input frequency and strong coupling.

The response function (Ψ) and firing rate responses (R) of the models suggest that the IF neurons have purely integrative properties. The RS neurons behave intermediately between integrators and resonators, having a quite rapid increase in firing rate as a function of input frequency and coupling. Finally, the RES model exhibits pronounced resonance, while having reliable responses for weak coupling and saturating for high coupling and high input frequency.

Excitability

To compare networks based on different neural models, one must first ensure that the level of excitability is similar across all networks. In other words, for the same network architecture but different models for individual neurons, we must have different synaptic strengths in order to obtain the same level of activity. To get a better understanding of the large differences in excitability, we stimulated the model neurons (IF, RS, RES) with a single afferent spike. The post-synaptic current is delivered once via an inhibitory synapse ($A_{syn} = 0.01$, $E_{syn} = -90$ mV, τ_{syn}

= 15 ms) and once via an excitatory synapse (A_{syn} *= 0.01,* E_{syn} *= 0 mV,* τ_{syn} *= 20 ms)*. For each model neuron, the hyperpolarization / depolarization of the membrane is recorded, relative to the resting potential. The peak of the membrane voltage excursion is computed as well, in order to give a quantitative estimate of the different levels of excitability.

The RES model is the most excitable, showing large oscillations of the membrane potential after stimulation (FIG. 4). At the other extreme, the RS neuron is much less excitable than IF and RES. For example, the peak of the depolarizing PSP of the RES model (*2.6 mV)* is more than 5 fold larger than in the case of the RS neuron *(0.51 mV)*. The weak response of RS neurons is explained by their low input impedance (FIG. 1).

Insert FIG. 4. about here.

An important observation has to be made here. Networks relying on different models of neurons are only comparable if the relative synaptic strengths are properly scaled to account for the excitability ratio between models. Since the two-dimensional reduced HH model for RS and RES neurons is highly nonlinear, we do not expect that the post-synaptic potentials would scale linearly as a function of the synaptic amplitude A_{syn}. Hence, we need to compute, for all synaptic amplitudes of interest, the actual ratio between the PSP peaks of the different models, to allow for a realistic calibration. As shown in FIG. 5, the RES model is exhibiting a strong nonlinear scaling in its response, relative to the RS model's response and a more moderate nonlinearity with respect to the IF model. At the same time, the IF-RS pair scales linearly, and has a constant ratio of excitability for all synaptic amplitudes.

Using the results in FIG. 5, one can calibrate the synaptic amplitudes for networks of IF, RS and RES neurons, such that the maximal PSP amplitude per afferent spike is roughly the same in all networks. However, due to different dynamical behaviors of the models to different input spike statistics, the calibration will not be perfect. The PSP is the same only if initially the

membrane is at rest. The actual PSP is also a function of the current state of the postsynaptic neuron and the scaling becomes somewhat imprecise for general neuron dynamics. Moreover, since the synaptic strengths in the network can take different values for different synapses, the real amplitudes of the post-synaptic currents that each neuron receives will be different (see eq. 5). This implies that the actual ratio of excitability for individual neurons might be different. Because of the nonlinear scaling between some of the models, a perfect calibration of the networks is not possible. Since we shall only compare networks with exactly the same architecture, we expect that such effects will not be dramatic. In general however, it is not clear how a perfect calibration could be achieved.

In any case, the plots in FIG. 5 show that the IF and RS networks can be properly calibrated, the IF and RES networks can be satisfyingly calibrated, while the RES and RS pair is the hardest to calibrate and hence to compare because of the nonlinear scaling of their excitability ratio.

For clarity purposes, throughout the rest of the paper, synaptic coupling strengths are reported relative to a reference, namely the coupling strength in RES networks (A_{syn}-RES). The coupling in the other networks is by default rescaled to obtain the same excitability level using results in FIG. 5 and the following formula:

$$A_{syn}IF\ or\ RS = A_{syn}RES \cdot \frac{Peak\_PSP_{IF\ or\ RS}}{Peak\_PSP_{RES}} \qquad (12)$$

where, the ratio between peak PSP amplitudes is reported in FIG. 5.

Insert FIG. 5. about here.

Microcircuits

In the following, we explored in what way the properties of individual neurons influence network dynamics. We investigated large networks of IF, RS and RES neurons also referred to as "neural microcircuits" (Maass et al. 2002; Grillner at al. 2005).

The investigated microcircuits consist of 1000 neurons, wired randomly with conductance based synapses (see Eq. 1 to 7). Among neurons, 80% are excitatory (IF, RS or RES) and 20% inhibitory (fast-spiking – FS – see Izhikevich 2003). Neurons have, on average, a 5% probability of synapsing with any other neuron in the network, such that the average number of synapses in the circuit is on the order of 50000. The wiring is non-homogeneous, in the sense that the number of afferent synapses per neuron varies, depending on the random instantiation. We also studied, as control conditions, homogeneous circuits, where the number of afferents per neuron is constant (only the identity of afferents is random) and also other connectivity ratios (2%, 3%, 4%).

The synaptic strengths (W_{syn}) are randomly drawn from a uniform distribution, taking values in the range (0..1]. The synaptic amplitudes (A_{syn}) are calibrated differently, depending on the experiment, as will be explained later. The networks are simulated using the "Neocortex" neural simulator developed by the authors (Mureşan and Ignat 2004).

There is a high degree of randomness involved in building such networks. The spatial distributions of excitatory/inhibitory neurons, the synaptic strengths, the connectivity patterns, are all randomly instantiated. Very different networks can be produced and these might exhibit very different behaviors. In the absence of any genetically guided architecture, our networks are just random guesses. Moreover, since the behavior of networks with different architectures can be dramatically different it becomes very difficult to generalize the observed phenomena. Nonetheless, our goal here is to compare how the firing property of individual neurons can yield qualitatively different network behaviors (FIG. 6). For this purpose, it is possible to compare networks that have the same architecture and differ only in terms of the neuron models used to build them.

Insert FIG. 6. about here.

To compare the networks' behavior that is induced by the different response properties of neurons, we always built 3 identical networks for each experiment. In each case, the networks have the same architecture, the only difference being the type of excitatory neuron used: IF, RS and RES, respectively. To ensure that the three networks are architecturally identical, once the synaptic connections for a network are instantiated, they are copied identically to the other two networks. In all three cases, the inhibitory interneurons are modeled as fast-spiking (FS) neurons (Izhikevich 2003). As mentioned, the three identical networks are instantiated for every experiment, such that an IF based network for example, is not the same in two different experiments (due to the random instantiation).

To calibrate the three types of networks, the amplitudes (A_{syn}) for excitatory and inhibitory synapses are rescaled. All excitatory synapses targeting an excitatory neuron, for example, share the same synaptic amplitude (the same is true for inhibitory synapses, but with a different synaptic amplitude value). The only difference between different synapses of the same type (excitatory or inhibitory) is their weight. Since A_{syn} for excitatory and inhibitory synapses are global parameters of the network, one is able to calibrate entire networks, by scaling them according to the described calibration technique (see section *Excitability* and *Eq. 5*).

Self-sustainability and stability

We first assessed the ability of different networks to produce self-sustained, *spontaneous activity* in the absence of any external input. Intuitively, a recurrent network is able to sustain its activity better (in the total absence of any external input), if the excitatory synapses are stronger. However, the stronger the synapses, the more likely it is that the network will be rendered unstable, eventually leading to "explosive" activity behavior (epileptic activity).

We investigated 2000 triplets of networks, each network in a triplet having the same architecture but different models for excitatory neurons (IF, RS and RES) and different scaling amplitudes for the synapses (A_{syn}). The architecture that is used to build a triplet is randomly instantiated, as described previously. In addition, we used another population of 100 input neurons, each connected randomly to 2% of neurons in the network.

For each triplet, the networks are tested for their ability to sustain *spontaneous activity* after a brief step-like input. The input is only used here for initializing the activity in the networks and is NOT to be considered an external event triggering *persistent activity*. The concept of *persistent activity* associates an external event / trigger that would change the already existing *spontaneous activity* to the specific multi-stable activity encoding the task (Miyashita and Chang 1988). Thus, even though there is an initial input, we are still studying *spontaneous* activity considering the input as a mere initialization of the network activities.

The input neurons were forced to spike, for 20 ms at the beginning of each trial, according to independent Poisson processes with a mean firing rate of 30 Hz. For the remaining 200 ms (the trial length is 220 ms), the networks evolve freely. For each network, we monitored the time dependent population firing rate (Π):

$$\Pi(t) = \frac{n(t, t+\Delta t)}{N \cdot \Delta t} \qquad (13)$$

where, $n(t,t+\Delta t)$ – is the total number of spikes in the network during the time interval $t \rightarrow t+\Delta t$; N – the number of neurons in the network (here 1000); Δt – the time bin used to integrate the model (here 10^{-3} s).

During 200 ms of free evolution without any input, we computed the time of activity survival for all three network types in a triplet, as a function of synaptic amplitude (FIG. 7a). The synaptic amplitude of the RES model is taken as a reference, while the amplitudes for IF and RS networks are scaled according to the scaling factors determined in section *Excitability* (see FIG. 5; both

excitatory and inhibitory synapses are scaled). The duration of activity survival is considered to be the duration of "normal" activity, until either a "die out" or an "explosive" event is detected. The "die out" event is defined as the moment in time after which the network does not fire any spike any more. The "explosive" event is considered to occur when the network starts firing at unusually high rates (more than 300 Hz) and maintains this high activity for at least 10 consecutive time bins (10 ms), indicating saturation. We also computed the percentage of networks that exhibit explosive behavior as a function of the synaptic coupling (FIG. 7b).

The results reported in FIG. 7a are averaged over 2000 triplets of networks. Each of the 2000 triplets is tested for all synaptic amplitudes, yielding a total of 20000 tests. As expected, the IF networks are the poorest in maintaining self-sustained activity. Regardless of the coupling strength, the IF-based networks' activity can only survive, on average, less than 30 ms after the ceasing of input stimulation. Their activity either dies out, or starts exploding very early, even for moderate synaptic couplings (FIG. 7b). The RS based networks are not significantly better in sustaining their activity as compared to IF networks. Over a certain threshold of the synaptic coupling, RS networks tend to become very unstable, most networks becoming "explosive" (FIG. 7b). This is partly due to the fact that synaptic amplitudes in RS networks are much higher than in the other 2 cases, as a result of the scaling to reach similar excitability (according to FIG. 5, RS excitatory synaptic amplitudes have to be almost 4 fold stronger than for the case of IF networks during calibration). The impedance of RS neurons, relatively constant over different input frequencies (FIG. 1), is also likely to play a role in such unstable behavior. Also worth noting is the very abrupt transition of IF and RS networks from stable to "explosive" dynamics (FIG. 7b).

Insert FIG. 7. about here.

The most interesting behavior is exhibited by RES networks. For very weak coupling, their activity does not survive after the ceasing of the input. However, for moderate coupling they start

sustaining more and more reliably their *spontaneous activity*, after the initialization phase (with input). There is a threshold-like transition from quiescent to self-sustained behavior, as suggested by FIG. 7a. The large standard deviation in FIG. 7a for a certain coupling (A_{syn}-*RES = 0.003*) indicates that some RES networks can sustain their activity for a long time, while for some others the activity dies out rather quickly, depending on the network architecture. For strong coupling however, the RES networks become deterministically self-sustained. They can robustly maintain their activity for as long as the experiment lasts (here 200 ms). Most RES networks with moderate and strong coupling can sustain their activity, usually infinitely long (Mureşan et al. 2005). Moreover, RES networks never displayed explosive behavior for the range of synaptic couplings considered here (FIG. 7b).

Since only the IF and RS networks have "explosive" activity regimes, we investigated next the dynamics of their population rate (*IT*), immediately before and after an "explosion" was recorded. We wanted to assess the dynamics of the "explosive" process, getting an insight into how the saturation of dynamics in the two types of networks comes about. We recorded the population rate starting 10 ms before and up to 10 ms after the "explosive" event was detected (FIG. 8). The threshold for "explosion" detection was 300 Hz, the event being validated only if the network remained over the threshold for at least 10 ms. In FIG. 8a, the IF and RS networks' population rates were averaged over all networks exhibiting "explosive" activity and all synaptic coupling strengths. The slope of the population rate increase is higher for IF networks than RS networks, indicating a faster activity buildup.

Next, we determined, for each synaptic coupling strength for which "explosion" occurs, the dynamics of the population rate for IF (FIG. 8b) and RS (FIG. 8c) networks. The coupling strengths reported are the reference synaptic strengths of the RES networks (A_{syn}-*RES*) like in

FIG. 7, while the IF and RS real coupling strengths (A_{syn}-*IF* and A_{syn}-*RS*) are rescaled according to FIG. 5, as discussed before.

Insert FIG. 8. about here.

The first observation is that the IF networks' activity becomes "explosive" for smaller reference couplings than RS networks (consistent with FIG. 7b). Furthermore, for the same reference coupling, the slope of the rate increase is significantly higher for IF networks (FIG. 8b and c). For example, at a reference coupling of A_{syn}-*RES=0.01*, the slope of population rate increase for IF networks is 233 Hz/ms, compared to only 183 Hz/ms for RS networks (although the real coupling strength is much higher for RS networks: A_{syn}-*RS = 0.05* compared to A_{syn}-*IF = 0.0153*).

At closer inspection, results in FIG. 8b, reveal even more interesting aspects. For weaker couplings, the population rates are relatively high 10 ms before the "explosive" event. This indicates a slower buildup of the activity. In such cases, a network must already have significant activity before "exploding", to be able to cross the threshold. Moreover, the population rate increases almost linearly in relatively low coupling regimes (A_{syn}-*RES = 0.04*) for IF networks and moderate coupling (A_{syn}-*RES = 0.06*) for RS networks. For strong coupling, both types of networks exhibit "explosive" activity that increases exponentially fast in the first few milliseconds (in spite of low initial activity), and then saturates giving rise to a sigmoidal-like "explosion curve" (FIG. 8b and c). The slope of the rate increase depends on the coupling strength. Coupling is thus a major factor determining how unstable a network is (FIG. 7b) and how fast its activity "explodes" (FIG. 8b and c).

To explain the behavior of the IF, RS and RES networks, we need to recall the response landscapes presented in FIG. 3. The IF neuron does not exhibit any particular frequency preference, acting more like a passive RC circuit. Low input frequencies make it hardly firing while high input frequencies produce vigorous firing. As a result, when IF networks get into low

activity regimes the neurons tend to fire even less, pushing the network into a cascaded ceasing of activity. On the other hand, when a group of IF neurons gets very active, it tends to entrain more and more neurons with it, producing an avalanche effect and leading to the saturation of the network. Since the slope of the rate increase for IF neurons is high (FIG. 3 top-right), "explosive" activity settles in very easily when coupling in the network is high enough. Inhibition cannot compensate for this, since inhibitory neurons represent only 20% of neurons in the network and have on average the same synaptic efficacies as excitatory synapses. If inhibitory synapses were rendered stronger the IF networks' activity would die out very fast. The commonly employed solution to this problem has been to reduce the excitatory coupling in the network and add some unspecific background current to excitatory neurons, such as to keep the network alive (Amit and Brunel 1997; Brunel and Hakim 1999; Latham et al. 2000; Plesser and Gerstner 2000; Hansel and Mato 2001; Roxin et al. 2004).

RS networks are somewhat more stable than IF networks for moderate coupling regimes. As their excitability landscape suggests (FIG. 3 middle-right), RS neurons tend to have a bit smaller slope of the rate increase, while being more responsive for low frequencies than IF neurons. However, for strong coupling, the RS networks become very unstable (FIG. 7b). This is probably due to the relatively high input impedance of the RS neurons in the high frequency range. The "explosion" mechanism is similar to that of IF networks, but the slope of the population rate increase is smaller (FIG. 8c).

Finally, RES networks are the most stable and able to sustain robust *spontaneous activity*. This is due to two key properties. First, RES neurons are easy to excite even for weak inputs (FIG. 3 bottom-right). When the activity in the RES network drops, it is still easy to reignite it, if a minimal group of neurons in the network is providing enough input to the others. Second, when the activity in the network builds up, RES neurons tend to get less and less responsive, as

indicated by their firing rate activity landscape (FIG. 3 bottom-right). Thus, RES neurons can maintain a stable activity regime that keeps the network alive. For moderate synaptic amplitudes, the RES neurons tend to settle into a preferred low coupling regime, with a firing rate of 30-50 Hz, matching the resonant frequency of the membrane (FIG. 1 and FIG. 3 bottom-left, low coupling resonant regime). If the synaptic coupling is increased, the RES networks can fire sustained at quite high rates (60-80 Hz) without becoming epileptic. We have to mention that RES networks are usually able to maintain their *spontaneous activity* for indefinitely long. Another interesting phenomenon is that the coupling with inhibitory neurons as well as the membrane resonance of RES neurons produces remarkable oscillatory activity (FIG. 6).

Two major factors influence the stability of the studied networks, namely the synaptic connectivity and the size of the network. Results reported here are taken for the case of relatively highly coupled networks (5%) and non-homogeneous connectivity (each neuron has a different number of afferents, depending on the random instantiation of the network). We have studied, as control conditions, networks with lower connectivity (2%, 3%, 4%) as well as with homogeneous (constant number of afferents per neuron, but randomly selected) and non-homogeneous architectures. All the reported results are qualitatively preserved with remarkable accuracy. Quantitatively there are differences that are expected. For lower connectivity, the thresholds for "explosive" activity of IF and RS networks, as well as the threshold for self-sustainability of RES networks are higher (expected, since lower connectivity is similar to scaling down synaptic efficacies). The activity of IF and RS networks has a lower probability of becoming "explosive", but their self-sustained time drops significantly. For smaller network sizes, the "explosion" thresholds increase while the self-sustained durations of IF and RS networks drop. Additionally, the transition from stable to unstable (IF and RS) and from quiescent to self-sustained (RES) regimes becomes less sharp compared to FIG. 7. This is because smaller networks with less

synapses have a more heterogeneous structure and behavior (some are more "explosive", some are less) yielding a smoother average compared to FIG. 7a and b.

A more important observation is related to the oscillatory behavior of the networks. It seems that homogeneous RES networks are much more prone for developing oscillations than their heterogeneous counterparts. This phenomenon is probably related to the homogeneous / uniform number of synapses per neuron in homogeneous networks, yielding a balance of excitation across the population and favoring the development of synchronized assemblies promoted by resonance. Revealing the exact mechanism for the development of such oscillations goes beyond the scope of the present study, however these results emphasize the importance of the network architecture.

Network excitability

A very important issue related to network dynamics is the response property to external stimulation. A well known property of visual sensory cortices is the pronounced response of cells to preferred visual stimuli, referred to as "ON-response" (Frazor et al. 2004).

We wanted to investigate next in what way the response properties of various types of neurons (IF, RS and RES) influence network responsiveness to external input. It is worthy of mentioning that the "ON-response" is a phenomenon related to the changes in firing rates of neurons immediately after stimulus onset, relative to the baseline *spontaneous activity*. To be able to study the response properties of various networks to external input, we needed to insure first that the networks exhibit *spontaneous* dynamics.

Since only RES networks are self-sustained without input, the only way to compare the responsiveness of all networks is to endow IF and RS networks with *spontaneous activity* as well. As outlined before, it is very difficult if not impossible to obtain IF and RS networks with stable *spontaneous activity* without external drive. We will next introduce a background current to these

two networks such that they would exhibit *spontaneous* dynamics, in line with the common practice (Brunel and Hakim 1999; Hansel and Mato 2001; Latham et al. 2000; Plesser and Gerstner 2000; Roxin et al. 2004).

The first requirement is that coupling strengths in IF and RS networks are weak enough to prevent "explosive" behavior (see FIG. 7b). We next chose weak synaptic couplings for these two classes of networks, respecting the excitability ratios in FIG. 5 (A_{syn}-IF_{exc} = *0.0009,* A_{syn}-IF_{inh} = *0.0014,* A_{syn}-RS_{exc} = *0.0035,* A_{syn}-RS_{inh} = *0.005*). Consequently, weak coupling leads to a fast loss of activity (FIG. 7a) and introduces the need for background current in order to enable *spontaneous*, ongoing activity. Each IF and RS neuron receives thus an additional, random background current at each time step, drawn from a uniform distribution between 0 and I_{max}. The total input current to an IF or RS neuron becomes now the sum of the synaptic and background currents.

$$I = \sum_{all\ synapses} psc_i + I_{bck} \qquad (14)$$

where, I – the input current to the neuron (see Eq. 1 and 2); psc_i – the postsynaptic current delivered by an afferent synapse i (the sum runs over all afferent synapses); I_{bck} – is the background input current, randomly drawn from a uniform distribution between $0..I_{max}$ at each time step (1 ms).

For the RES networks an intermediate coupling (A_{syn}-*RES = 0.003*) is chosen such that the network would maintain a robust self-sustained activity that is usually in the range dictated by the resonant frequency for RES neurons (30-50 Hz). The background current amplitudes for IF and RS networks were adjusted during a calibration phase, such that the spontaneous population rates (Π) of these networks would closely match the reference RES population rate, with a tolerated error of ±5%. On average, the background current amplitudes of IF and RS networks required to attain the reference firing rate were I_{max}-*IF = 4.73 nA* and I_{max}-*RS = 27.30 nA*, respectively. The

calibration indicates that RS networks required even more input current relative to IF networks than predicted from FIG. 5. We need to keep this in mind, since it indicates that RS networks receive on average even more background noise, relative to IF networks, for the same spontaneous firing rate.

After calibration, all three networks maintain ongoing activity at the level of approximately 30-40 Hz. Such a high frequency is not quantitatively matching the spontaneous firing rate of cortical networks that is about 1-5 Hz (Amit and Brunel 1997). However, we were interested here in activity regimes where RES networks can robustly self-sustain activity in the absence of any input. For the particular model used in this study, the range is around 30-60 Hz. In any case, a direct quantitative comparison to cortical dynamics would be tentative and speculative.

Following a period of stabilization of activity, the networks are stimulated using a population of 100 input neurons that project to all three networks. The input connections of the networks are structurally identical, while the synaptic amplitudes are calibrated to address the excitability issue discussed in section *Excitability*. Hence, all networks receive the same stimulation pattern. The networks are stimulated for 50 ms with a Poisson input of 20 Hz (see FIG. 9a). Then, they are allowed to freely evolve for another 1450 ms, after which the process is repeated. Each such 1500 ms interval represents a trial. During the trial, we recorded the population rates (*II*) and average membrane potentials.

Insert FIG. 9. about here.

We investigated the response properties to input by averaging the population rates over 100 trials, aligned to the beginning of the trial (similar to Peri-Stimulus Time Histograms - see Gerstner and Kistler 2002), for 50 networks of each type. Results shown in FIG. 9a suggest that the most responsive network is by far the IF-network. Because of the rather strong depolarizing background current required for *spontaneous activity* and the internal network bombardment, IF

neurons have an average membrane potential of -53.69 mV (FIG. 9b), between the resting potential of -70 mV and the threshold of -45 mV. This phenomenon probably leads to a so-called "high conductance state" in which neurons become more responsive to input as the slope of the gain function is modulated (for a review, see Destexhe et al. 2003). Please note that even though we use a linear leaky integrate-and-fire model, the conductance based model of the synaptic currents yields an "effective membrane conductance" that is modulated by the depolarization level of the neuron, giving rise to the "high conductance state" (Rudolph and Destexhe 2006).

Both the "high-conductance states" as well as recurrent self-excitation of subgroups of neurons could be the cause for such a robust response of IF networks to input. As indicated in FIG. 8a and b, for strong coupling and without background current, the recurrent excitation produces rapid activity buildup that is hardly compensated by inhibition. This indicates that the recurrent groups are a major source for such a high responsiveness. Furthermore, the relatively slow convergence of the population activity back to the baseline of 30 Hz (FIG. 9a) suggests that activity is reverberating for a while, due to these intrinsic recurrent groups in the network.

Although RS networks are bombarded with background currents more than 5.5 fold larger in amplitude compared to IF networks, they tend to be much less responsive. As the excitability landscape in FIG. 3 middle-left suggests, RS neurons have some weak resonance properties and tend to dampen high input frequencies in suprathreshold regime. In the subthreshold regime, for low frequencies, RS neurons have relatively reduced input impedance (FIG. 1). These properties probably impair or slow down the formation of recurrently excited groups, for *weak coupling* in the network (consistent with FIG. 7b). Moreover, RS networks display a rapidly decaying tonic response followed by a very prominent dip in the activity after the stimulation ceases (FIG. 9a). The latter phenomenon might be related to the adaptation properties of RS neurons (Izhikevich 2003) and is clearly reflected in the hyperpolarizing phase of the average membrane potential

trace (FIG. 9b). Adaptation is likely to be involved also in the progressive reduction in response during the stimulation (FIG. 9a, from 20 to 50 ms). Overall, the effect of the input stimulation is maintained for quite a long time, close to that of IF networks (FIG. 9a, from 0 to 120 ms), although it consists of both an excited and a hyperpolarized phase.

RES networks are the least responsive, having a quite weak response to input stimulation. The firing rate of such networks increases less, relative to IF or RS networks, albeit the effective input drive is similar (calibrated based on FIG. 5, as mentioned before). Moreover, the effect of stimulating RES networks quickly vanishes after the stimulation is removed (they return close to the baseline level almost simultaneously with the ceasing of the input, displaying a dampened oscillation arround baseline – see FIG. 9a). This indicates a high reluctance of RES networks to rate changes induced by the stimulus. They have low responsiveness to input and exhibit fast re-stabilization of the activity to the homeostatic baseline level. Altogether, such evidence suggests that RES networks are prominently homeostatic, with very stable activity, however reluctant to external drive.

Activity patterns

The patterns of activity in the three types of networks are dramatically different as suggested also in FIG. 6 (in spite the fact that they have the same architecture). We wanted to assess the relation between the response properties of IF, RS and RES neurons and the resulting activity patterns that are produced by the three types of networks. We considered the same protocol as presented in the previous subsection *Network excitability*, with triplets of networks firing at a baseline level of about 30-40 Hz and being stimulated with 20 Hz Poisson inputs lasting 50 ms. In each trial, we monitored, in addition to population rates and average membrane potentials, also

the population inter-spike interval (ISI) randomness, a new measure that we introduced in order to characterize the activity patterns in the networks.

Insert FIG. 10. about here.

The population ISI randomness (S_{ISI}) measures the degree of disorder in the ISIs of a population of neurons during a given time window. In some sense, the S_{ISI} is similar to the concept of entropy. We defined the population ISI randomness as follows (see also APPENDIX). The spikes of a population of neurons are recorded in a sliding window of 150 ms. All ISIs of all neurons in the window are computed and we denote the total number of ISIs with N_{ISI}. N_{ISI} depends both on the number of neurons considered as well as on the number of spikes they fired within the time window. Next, the values of ISIs are clustered such that each cluster contains all ISIs that are within a range of ±10% of the value of the cluster center. A number Nc_{ind} of independent clusters is determined (see APPENDIX for details). The population ISI randomness indicates the fraction of independent clusters relative to the total number of ISIs.

$$S_{ISI} = \frac{Nc_{ind}}{N_{ISI}} \tag{15}$$

In other words, S_{ISI} shows how many independent values of the ISIs (with a tolerance of 10%) are required to describe the whole window, for all neurons. One could see it as a ratio of information compression. If all neurons were firing with the same ISI (for example being aligned to a common oscillation cycle), one number would be enough to represent all the ISIs in the window and S_{ISI} would be the lowest ($1/N_{ISI}$). If each neuron fired with a different ISI at different moments such that all ISIs in the window were significantly different, the randomness measure would approach a value of 1.

The advantage of the population ISI randomness measure is that it is able to quantify the degree of disorder in the activity of a population of neurons, independently of the ISI distribution. Other techniques of estimating the degree of randomness, like computing the coefficient of variation *Cv*

(Softky and Koch 1993), deal only with one neuron at a time and are only applicable if the ISI distribution is unimodal. The RS and RES networks frequently engage in oscillatory behavior such that the ISI distributions can be bimodal (one peak for the inter-cycle distance and one peak for the in-cycle bursting). In some sense, the population ISI randomness would correspond to computing the coefficients of variation in different sub domains of the ISI distribution that are centered upon the local peaks of the distribution.

The disadvantage of the population ISI randomness measure is that it is influenced by the firing rate. Even for stationary firing processes, a higher firing rate yields a lower randomness, because of the clustering of ISIs that is more precise for smaller values of ISIs. Since our three networks fire with the same spontaneous rate, the comparison of the three S_{ISI} values is not affected by this issue during the stationary non-stimulated phase (FIG. 10a).

After the initial stimulation phase, the networks undergo severe reorganization. This is reflected by the change in S_{ISI}, depicted in FIG. 10a. As mentioned before, because of the strong rate increase, the ISI population randomness decreases in all cases since ISIs get smaller. However, after this non-stationary phase, networks get back to the stationary *spontaneous activity* during which S_{ISI} is constant. Interestingly, the IF networks have the highest stationary ISI randomness, even though RS networks have the strongest background random drive (recall the remark from the calibration of input currents to provide spontaneous activity in IF and RS networks). This indicates that IF neurons are not capable of coupling into preferential firing patterns, unlike RS neurons which can take advantage of their adaptation and weak resonant properties to produce preferential ISI intervals and can couple into robust oscillatory firing patterns (FIG. 6). As expected, RES networks have the lowest ISI randomness because there is no random background current and because neurons have preferred ISIs due to their membrane resonance, inducing a highly ordered activity (FIG. 6).

We also computed the ISI distributions of IF, RS and RES networks during the stationary phase of a trial. IF networks have the highest spread of the ISI distribution (FIG. 10b), indicating the highest disorder, just as predicted by the ISI population randomness. The ISI distribution of RS networks is more compact and less spread (FIG. 10c) because RS neurons fire more regularly than their IF counterparts. In the case of the RES networks, the precision of firing is remarkable, neurons having preferred ISIs (FIG. 10d) in the range of 25-40 ms, close to the period of subthreshold membrane oscillation (FIG. 4) and consistent with their frequency preference (FIG. 1).

The ISI population randomness and ISI distributions suggest that resonant properties endow a network with more regular and precise firing, favoring the onset of oscillatory activity. On the other hand, integrative properties endow a network with more degrees of freedom, enabling it to accommodate random patterns of activity.

Relationship with other mechanisms contributing to stable spontaneous activity

So far we have investigated in what way the membrane properties of network neurons influence the stability of reverberating microcircuits, their responses to stimulation and their patterns of activity. We next considered other potential mechanisms that can contribute to stable *spontaneous activity* of microcircuits. First, we investigate the importance of miniature synaptic potentials in providing a "lower bound" for the activity of RS circuits. Then, we search for other potential sources of stability providing the "higher bound" of network dynamics, such as synaptic delay mechanisms.

Miniature synaptic potentials (minis). Following a previous study of Timofeev and collaborators (see Timofeev at al. 2000) and recent evidence about the properties of minis (Paré et al. 1997, 1998) we next considered the RS circuits used in section "*Self-sustainability and*

stability" and added one extra excitatory synaptic conductance to each RS neuron (mini conductance). To simulate spontaneous release, the mini conductances are changed (increased), on average with a frequency of 20 Hz (see Paré et al. 1997). Each spontaneous conductance increase has amplitude that is randomly drawn from a uniform distribution with a maximum specified value $\Delta g\text{-}max$ (in Eq. 7, for the case of mini conductances, g is increased with a random amplitude having a specified maximum of $\Delta g\text{-}max$ = 8, 8.5, 9, 9.5, 10, depending on the experiment). The mini conductance parameters have been chosen such that the amplitude of mini PSPs was in the physiological range of 0.1 to a few millivolts ($A_{syn}\text{-}mini = 0.0035$ *uS,* W_{syn} is randomly drawn from a uniform distribution with a mean of 1.56 ± 0.88, $\tau_{syn} = 10$ *ms,* $E_{syn} = 0$ *mV*). Each network is simulated for 100 seconds (10^5 steps) and results are averaged across 50 random networks.

Insert FIG. 11. about here.

Two crucial parameters influence the behavior of these networks: the coupling strength within the network ($A_{syn}\text{-}RS$) and the average amplitude of the mini PSPs (controlled by $\Delta g\text{-}max$). For weak coupling and small amplitude of minis, the RS networks fire in a tonic fashion with very low firing rates (0.2 to 0.9 Hz), dependent on the amplitude of the minis (FIG. 12b). As the coupling in the network is increased, for a relatively narrow range of parameters ($A_{syn}\text{-}RS \in [0.02..0.03]$), the activity becomes bursty (FIG. 12c), with high peaks of the population rate and burst-like firing of RS neurons (FIG. 11). If the coupling is further increased, the RS networks become "explosive", just as reported before in FIG. 7b. Please note that the coupling values for the transition from tonic to bursting regimes correspond to the critical region of transition from "dying out" to "explosive" behavior of the RS networks in FIG. 7b (corresponding to a reference $A_{syn}\text{-}RES$ between 0.04..0.07).

Insert FIG. 12. about here.

At the onset of burst-like firing, the bursts occur rather irregularly with very long inter-burst intervals (on the order of tens of seconds) and have low amplitudes (computed from the population rate). As the network coupling is increased, bursting becomes more reliable and has higher amplitudes (FIG. 12c, d and e). If, in addition the amplitude of minis is increased, the bursting process becomes more and more periodic (FIG. 12g and h).

There are several interesting observations. First, although the mean population rates (FIG. 12a) increase rapidly with increasing network coupling and mini amplitude, the mean baseline population rates (not including the bursts) increase steadily and much slower (FIG. 12b). This indicates that the average network activity, excepting the bursts, scales slowly with network coupling and mini amplitude. The network activity becomes high only in the vicinity of bursts indicating a "runaway-like" recurrently-amplified, self-excitation process that is network dependent. This argument is supported even further by the fact that the burst amplitude does not seem to depend on the amplitude of the miniature PSP's. In FIG. 12d and e, the means of the burst amplitude distributions, for the same coupling but different mini PSP amplitudes, are very close to each other. The means of these means and their standard deviations are shown in FIG. 12f computed for the three couplings where bursting occurs (0.025, 0.0275, 0.03), across all mini PSP amplitudes. The mean burst amplitudes increase linearly and their standard deviation (computed across different mini amplitudes) is small. On the other hand, the number of bursts for the same coupling strength depends critically on the mini PSP amplitudes (see the dependency of the size of the distributions in FIG. 12d and e on the mini amplitudes).

These results suggest that the bursting of the network is not driven (although it might be initiated) by a chance synchronous accumulation of miniature PSPs but is rather a recurrent activity self-amplification process that is network dependent. The burst process is a property of the network and this is consistent with previous findings (Timofeev et al. 2000). The amplitude of

miniature PSPs, on the other hand, influences the probability that the network will burst and, in addition, whether this bursting is periodic (FIG. 12g and h). The position of the peak of the inter-burst interval (IBI) distributions does not seem to depend on the network coupling but only on the mini PSP amplitudes. The sharpness of this peak is however modulated by the network coupling (FIG. 12g and h).

To summarize, depending on the values of the two critical parameters (network coupling and mini PSP amplitudes) RS networks can produce three activity regimes: tonic, aperiodic bursting and periodic bursting (FIG. 12i). The bursting and its dynamics (amplitude) are properties of the network, while the probability of initiating a burst and the periodicity of bursts depend on the amplitudes of the miniature synaptic potentials. Finally, the spike-frequency adaptation of RS neurons is very likely to be involved in extinguishing these bursts and preventing "explosion", for the narrow coupling, at the threshold between stable and "explosive" dynamics.

Synaptic delays. We investigated next the influence of synaptic delays on the networks described in section "*Self-sustainability and stability*". We considered exactly the same type of networks and experimental setup and additionally introduced synaptic delays. We defined a maximum propagation delay for the most distant pair of neurons, ranging from 20 to 100 ms. Resonant networks remain very stable and become self-sustained even earlier than shown in FIG. 7, for a reference coupling of A_{syn}-*RES = 0.001*.

Insert FIG. 13 about here.

The self-sustained duration of IF networks' activity does not seem to be significantly modulated by delays (FIG. 13a) and, although there is a weak trend towards longer self-sustained durations, there is no dramatic improvement compared to the "no delay" condition (see FIG. 7a). On the other hand, the RS networks' self-sustained durations are significantly modulated by synaptic delays (FIG. 13b). For relatively long propagation delays, they can sustain activity up to

the entire experiment duration (200 ms). However, we have to mention that this phenomenon is by no means comparable in robustness to the self-sustained regime of resonant networks, which can sustain activity for indefinitely long periods.

Regarding "explosive" behavior, IF and RS networks become less "explosive", hence more stable, and the synaptic coupling for which runaway activity occurs is strongly modulated by the amplitude of synaptic delays (FIG. 13c and d). Longer delays favor more stable dynamics and the "explosive" process progresses slower (the slopes of the population rate increase during "explosion" are smaller than those in FIG. 8).

Our results suggest that integration alone cannot take full advantage of synaptic delays in maintaining robust ongoing activity, except for the fact that IF networks become less "explosive". The excitation in the network is quickly lost by integrator neurons because of a temporal spread of action potentials due to delays, which impairs synchronization and affects integration. Probably other additional factors would be required, such as long synaptic time constants, corresponding to NMDA mediated neurotransmission, for example. In contrast, RS networks' activity is much stronger modulated by synaptic delays. The frequency adaptation and weak resonant properties of RS neurons, together with the synaptic delays that prevent "explosion", allow RS networks to become quite robustly self-sustained. As a final conclusion, synaptic delays provide a robust "upper bound" of activity by preventing activity "explosion". However, they are not sufficient to stabilize the "lower bound" of network activity in general, for which the membrane properties of the neurons become crucial.

DISCUSSION

We have shown that the response properties of different neural models can dramatically influence the behavior of networks based on such models. In particular, we have studied two basic properties of the membrane dynamics: integration and resonance. We discussed how different models have very different behavior in terms of excitability and response property as a function of the temporal structure of the input spike trains. At one extreme, the integrate-and-fire model prefers high frequency inputs and shows no adaptation. At the other extreme, resonant neurons have preferred input frequencies, dampening high input bombardment while being quite sensitive to weak inputs. This property has important consequences for the homeostasis of network activity. We outlined the ability of networks built with resonant neurons to robustly maintain *spontaneous activity* in the absence of any stimulation. In turn, this homeostatic regime impairs the responsiveness of resonant networks to external stimulation. We concluded that resonance facilitates the stability of network dynamics at the cost of sacrificing responsiveness, while integration provides reliable responsiveness but sacrifices stability.

Additionally, we investigated the relationship between membrane properties and other processes potentially contributing to stable *spontaneous activity*: miniature synaptic potentials and synaptic delays. Miniature synaptic potentials can endow networks of regular spiking neurons with *spontaneous activity.* The spike-frequency adaptation of these neurons together with recurrent excitation lead to burst-like firing, often observed *in vivo* during slow-wave sleep states (Steriade et al. 1993; Timofeev et al. 2000; Steriade 2006). The bursting is a property of the network while the number of the bursts and their periodicity depend on the amplitude of mini PSPs. Regarding synaptic delays, we have shown that they can provide an upper bound on neural activity, preventing “explosive” dynamics. However, even with synaptic delays, membrane

properties become essential for providing stability at the "lower bound" of neural activity and allowing network reverberations to sustain ongoing dynamics.

Generality of results

The present study relies on specific models of neurons and it should be made clear that there is no attempt here to model brain activity quantitatively. The IF model is probably the most popular and is used for large-scale simulations of neural microcircuits, being well known for its purely integrative properties. The Izhikevich RS and RES models exhibit other interesting dynamical behaviors like adaptation and resonance, being relevant to our discussion. We explicitly studied the properties of these specific models and there is no guarantee that they would directly translate to the brain. For example, the *spontaneous* firing rate attained by our resonant networks was in the range of 30-50 Hz, rather incompatible with the 1-5 Hz *spontaneous activity* of the cortex. It could be suggested that such an elevated firing rate would be more appropriate to account for *persistent* rather than *spontaneous activity*. However, *persistent activity* involves multi-stability (Durstewitz and Seamans 2006), such that the sustained activity pattern could be switched on or off. In our case, the resonant networks maintain their activity in a *homeostatic* manner, and there is no multi-stability involved. The *spontaneous* firing rate of our resonant networks is stable around 30-50 Hz because of the particular choice for the model that resonates at such high frequencies. It is known however that thalamo-cortical neurons can display resonance at low frequencies as well (Hutcheon and Yarom 2000). This low frequency resonance (1-2 Hz) matches well the *spontaneous* firing frequency in cortical networks (1-5 Hz).

Regarding the RS model, we have to mention that the classification into spiking classes has been done according to the response of cells to step input currents. In the cortex, cells can often change their firing properties such that regular-spiking cells can become intrinsically-bursting

during sleep or anesthesia (Timofeev et al. 2000). The fact that in our model, RS cells have weak resonant properties and that in the cortex pyramidal cells are often regular spiking cells should not be considered as evidence that excitatory neurons in the cortex do not resonate. Actually, real cells can switch between different dynamical modes and the pyramidal neurons (sometimes classified as RS cells) can display resonant behavior (Hutcheon and Yarom 2000; Fellous et al. 2001). The types of neurons used in our simulations are "toy models" compared to the complexity and versatility of biological neurons. No direct correspondence should be made between our model neurons and cortical neuron types.

Nonetheless, since most of our results are rather qualitative, based on comparing different networks, the presented findings become general enough to allow for meaningful conclusions. We only compare how integration and resonance would affect the activity of otherwise identical networks of spiking neurons and show that these two properties endow large-scale neural circuits with very different dynamical behaviors. We have to mention that the presented phenomena were remarkably robust for all network architectures and sizes that we tested. For the case of resonant networks, we show that robust self-sustained activity can be attained in the absence of any external stimulation. We are not aware of any other study showing that such robust ongoing activity can be produced in artificial neural microcircuits without background input. This opens new possibilities for studying completely deterministic networks whose *spontaneous activity* is solely maintained by the interactions in the network.

Membrane properties, network dynamics and cortical processes

As we have seen, the membrane properties of neurons in large networks dramatically determine their behavior. Integration and resonance endow networks with responsiveness and versatility on one hand and temporal precision and stability on the other, respectively. But other neural

properties that stem from membrane dynamics, such as spike-frequency adaptation, can contribute to the production of specific patterns of network activity. For example the adaptation and the intermediate response property (between integration and resonance) of RS neurons lead to oscillatory network bursting under the influence of miniature synaptic potentials. Moreover, various network properties such as synaptic delays, have differential effects depending on the membrane properties of the constituent neurons. In our study, we have shown that in spite of strong network coupling and synaptic delays, purely integrative networks are not able to sustain activity for long durations, as opposed to RS networks that take advantage of both. In the context of the homeostasis of network activity, there are probably many more, other relevant processes, acting on multiple levels, from synapses to global neuromodulation. They are differentially expressed during various cortical states and their interaction is most likely non-trivial. It remains a future challenge to investigate the role of each such process individually and even more so, in a collective framework.

There are several remarks that have to be made, before concluding this study. First, neurons were considered for a long time to behave as integrators and this is reflected by the overwhelming number of studies based on the integrative paradigm, especially in modeling. Other properties of neurons, like resonance, have only relatively recently been emphasized and explicitly explored. In the experimental field there is accumulating evidence that real neurons have rather pronounced resonant properties. Resonance has been found in the somatosensory cortex (Hutcheon et al. 1996; Ulrich 2002), prefrontal cortex (Fellous et al. 2001), entorhinal cortex (Erchova et al. 2004; Schreiber et al. 2004), thalamus (Puil et al. 1994), hippocampus (Leung and Yu 1998) and interneurons (Pike et al. 2000). It has been suggested that resonance could play an important role in selective communication between neurons (Izhikevich 2002) and that neurons can communicate their frequency preference to post-synaptic targets leading to a

complex interplay with their firing rate (Richardson et al. 2003). It was also shown that the intrinsic properties of the cellular membrane could have a major impact on frequency-dependent information flow in the hippocampus (Erchova et al. 2004). Taken together, these facts emphasize the importance of resonance in neural circuits. In addition, we suggested here that resonance could play a very important role in the homeostasis of network activity and that it affects quite significantly the response properties of recurrent networks to input stimulation.

Second, there is rapidly accumulating evidence that neural systems posses homeostatic regulatory mechanisms, spanning several levels of organization (Turrigiano and Nelson 2004; Davis 2006). Such regulatory processes can act at the level of synapses as well as within the cell itself, changing its global properties. They can be slow (intrinsic plasticity, synaptic scaling) or relatively fast (short-term plasticity, spike-frequency adaptation). To the best of our knowledge, resonance has not yet been explicitly suggested to play a homeostatic role in regulating network activity. As we have shown here, resonance can dramatically contribute to the stabilization of network dynamics and we suggest that it could be a very robust homeostatic mechanism. Resonance is a global property of the cell's response (not local, like synaptic mechanisms) and it is fast. We also have to mention that the homeostatic regulation of network dynamics through resonance is more a passive process as opposed to the common notion that homeostasis is an active process involving the change of cellular and synaptic properties over time (Turrigiano and Nelson 2004).

Third, resonance at the membrane level can facilitate networks to engage into oscillatory behavior. Neurons with the same preferred inter-spike intervals tend to periodically lock into coherent oscillatory patterns. We also find that resonant networks display marked oscillations (FIG. 6) and our observations are consistent with the idea that intrinsic membrane properties

dramatically affect the ability of networks to produce oscillatory patterns of activity (Lampl and Yarom 1997; Hutcheon and Yarom 2000; Geisler et al. 2005; Buzsáki 2006).

A very important aspect related to resonance is that it can be modulated. Recent studies suggest that resonant behavior is voltage-dependent. For example, cortical pyramidal neurons have two resonant frequencies (1-2 Hz and 5-20 Hz), depending on the level of depolarization of the cell (Puil et al. 1994; Hutcheon et al. 1996; Lampl and Yarom 1997; Hutcheon and Yarom 2000). This finding is very important for the following reason. On one hand, it has been suggested that resonance underlies oscillatory behavior in cortical networks. On the other hand, there is accumulating evidence for the association between neural oscillations and attention (Fries et al. 2001). It is possible, in principle, that attention-related oscillations can be produced by modulating resonance via adjustment of the average membrane potential. Similar suggestions, but in a different form, have been made by Bazhenov et al. (Bazhenov et al. 2005) who proposed that resonant properties together with synaptic coupling can contribute to the control of information flow in cortical networks. The finding that robust oscillations can be mediated by resonance calls for future investigations of the complex interplay between membrane potential, resonance, oscillatory behavior on one side, and attention, on the other.

Fourth, our results suggest that resonance induces more temporally structured activity than integration, at the expense of reluctance to external stimulation. Even with significantly high external noise, neural adaptation and resonance allow a network to produce more regular firing (RS in FIG. 10). Increased reliability of firing relying on membrane resonance phenomena have also been described experimentally (Fellous et al. 2001) and theoretically (Bazhenov et al. 2005). Since resonance restricts the degrees of freedom for the firing of neurons, external stimulation causes temporal reorganization rather than firing-rate response in resonant networks (FIG. 9a). Conversely, networks featuring pure integration are very sensitive to external excitation and

respond with increased firing rate. They are more prone to firing-rate signaling and exhibit less temporally organized activity (FIG. 9 and FIG. 10). These observations hint towards two different ways of representing information in cortical networks that could be supported by resonance and integration: temporal versus firing-rate coding.

The more temporally structured firing of resonant networks can be related to other important aspects. It was recently found that homeostatic mechanisms play a crucial role in the developing nervous system, regulating *spontaneous activity* (Turrigiano 2006; Turrigiano and Nelson 2006). However, it is not only the level of *spontaneous activity* that is important, but also the spatiotemporal patterns of activity produced therein (Torborg and Feller 2005; Turrigiano 2006). Our findings suggest that resonance can be involved both in maintaining homeostatic *spontaneous activity* and in shaping the spatiotemporal structure of the network dynamics.

Furthermore, as we have seen, resonant neurons can fire at remarkably regular intervals (FIG. 10d). Such regular firing patterns have been observed already in the pyramidal tract, in the early studies of Evarts (Evarts 1964). Interestingly, later it became generally accepted that neurons in the cortex fire rather irregularly (Tuckwell 1989; Softky and Koch 1993) but recently the regularity of firing was shown to depend on the cortical state, as well as on the optimality of driving the neurons (Gur and Snodderly 2006). Since there is evidence that resonance can be modulated in a voltage-dependent way, we suggest that cortical neurons might switch between resonant and integrative behavior as their membrane potentials are influenced by the cortical state. As it was shown in our study, these two properties could induce regularity or randomness, respectively, in the activity of recurrent microcircuits.

Finally, we believe that integration and resonance are two different mechanisms that might be functionally relevant to the cortex. Integration is favorable to processing rate codes and promotes high sensitivity of recurrent networks to inputs. At the other extreme, resonance contributes to the

homeostasis of network dynamics and supports more temporal-like codes, while promoting oscillatory behavior. These two mechanisms might interact in the brain to produce dynamics that are complex and sensitive to inputs, yet stable. In general, as we have seen in this study, membrane properties of neurons determine to a large extent how various processes influence network dynamics. The equation involving voltage-dependent resonance, integration, homeostasis, excitability, oscillations, attention, activity patterning and many other phenomena is likely to be complex, but deserves thorough and sustained future investigations.

APPENDIX

We present in more detail the algorithm used to compute the population ISI randomness, S_{ISI}. Let us consider a population of 3 neurons that fire spikes quite randomly, with ISIs given in APPENDIX FIG. 1.

Insert APPENDIX FIG. 1. about here.

To compute the population ISI randomness at time t using a sliding window of 150 ms, the first step is to compute the ISIs of neurons for the window centered at time t. Next, using all the ISIs in the window, a population ISI histogram (H_{ISI}) is computed (it takes all ISIs from all neurons). An example histogram is depicted in APPENDIX FIG. 1 (bottom). We use a 1 ms bin to compute the histogram.

Based on H_{ISI}, we compute the number of independent ISIs by clustering ISIs into groups that are spanning 10% the value of an ISI cluster center. The clustering algorithm, described below, sequentially iterates H_{ISI} and tries to determine if, for the current ISI, there is an already determined cluster center (with a lower ISI value) that is less than 10% apart from it. If such a cluster is found, then the ISI belongs to the previous cluster, otherwise it becomes the center of a new cluster. The algorithm then moves to the next ISI and repeats the same procedure, until all the H_{ISI} has been analyzed. We obtain a number of ISIs that are independent from each other (Nc_{ind}) within 10% of their respective values. For example, a cluster having a center at 20 ms, would contain all ISIs between 20 and 22 ms, while a cluster with the center at 100 ms would contain all ISIs between 100 and 110 ms.

The final value of S_{ISI} at time t is the ratio between the number of independent ISIs and the total number of ISIs (see APPENDIX FIG. 1).

The exact algorithm given below:

Variables:

$H_{ISI}[]$	Array containing the histogram of ISIs, with a bining of 1 ms
N_{ISI}	Total number of ISIs in the window
Nc_{ind}	Number of independent clusters
last	Auxiliary variable used to memorize the position of the last computed cluster center
W_{ISI}	Window size used to compute S_{ISI}
found	Flag variable checking if any non-zero ISI count value $H_{ISI}[k]$, is found at k between 0.9*i and i-1, where i is the value of the ISI being probed
left	Starting index for counter k (taken 0.9*i)
right	Ending index for counter k (taken i-1)
S_{ISI}	The population ISI randomness

Algorithm (computes S_{ISI} for a given window of size W_{ISI}):

```
Compute H_ISI;
N_ISI  := 0;
Nc_ind := 0;
last := -1;

FOR i:=1 TO W_ISI DO
   IF(H_ISI[i] > 0) THEN
      //Set the bounds to search for a cluster center smaller than i
      found := FALSE;
      left := Round(0.9*i);
      right := i-1;
      //Try to find an ISI smaller than i, within 10% of i
      FOR k:=left TO right DO
         IF(H_ISI[k] > 0) THEN found := TRUE;
      ENDFOR;
      //If an ISI is found, but it is not a cluster center
      IF((found) AND ((i-last)>(i-left))) THEN
         found := FALSE;
      ENDIF;
      //Make a new cluster center if a smaller one was not found
      IF(NOT found) THEN
         Nc_ind := Nc_ind + 1;
         last := i;
```

```
      ENDIF;
      //Integrate the H_ISI to compute N_ISI
      N_ISI := N_ISI + H_ISI[i];
   ENDIF;
ENDFOR;

S_ISI := Nc_ind / N_ISI.
```

The algorithm searches for ISIs that occur in the window (they have $H_{ISI} > 0$). For each ISI, i, it tries to determine whether there is a cluster center already determined, within less than 10% of i, smaller than i. If such a value exists, and it is a cluster center, then i belongs to the last computed cluster denoted by *last*. If no such value is found, then i is an independent cluster center, and Nc_{ind} is incremrented, *last* being moved to i. Additionally, the algorithm computes the total number of ISIs (N_{ISI}) in the window by integrating the histogram H_{ISI}.

Finally, the S_{ISI} at moment t is computed by dividing the number of independent clusters by the total number of ISIs. The window is shifted by 1 ms forward and the procedure is repeated for moment $t+1$. The time-resolved S_{ISI} (FIG. 10a) is obtained by computing S_{ISI} for each moment in time spanning a trial.

ACKNOWLEDGEMENTS

The authors would like to thank Danko Nikolić, Wolf Singer, Răzvan V. Florian, Eugene M. Izhikevich, Vlad V. Moca, Adrian Iftime, Ovidiu F. Jurjuţ, Jochen Triesch and Iosif Ignat for useful comments on the earlier versions of the manuscript and interesting discussions.

GRANTS

Raul C. Mureşan and Cristina Savin gratefully acknowledge the financial support from the Hertie Foundation.

REFERENCES

Abbott LF and Nelson SB. Synaptic plasticity: taming the beast. *Nature Neuroscience* 3:1178–1183, 2000.

Abbott LF and Regehr WG. Synaptic Computation. *Nature* 431:796-803, 2004.

Amit DJ and Brunel N. Model of Global Spontaneous Activity and Local Structured Activity During Delay Periods in the Cerebral Cortex. *Cerebral Cortex* 7:237-252, 1997.

Arieli A, Shoham D, Hildesheim R, Grinvald A. Coherent spatiotemporal patterns of ongoing activity revealed by real-time optical imaging coupled with single-unit recording in the cat visual cortex. *Journal of Neurophysiology* 73(5):2072-93, 1995.

Arieli A, Sterkin A, Grinvald A, Aertsen A. Dynamics of ongoing activity: explanation of the large variability in evoked cortical responses. *Science* 273:1868-1871, 1996.

Arieli A. *Ongoing activity and the "state of mind": the role of spontaneously emerging cortical states in visual perception and motor action*. Workshop "Electrophysiological Semiotics of the Neuronal Systems", Warsaw, Poland, 2004.

Bazhenov M, Rulkov NF, Fellous JM, Timofeev I. Role of network dynamics in shaping spike timing reliability. *Physical Review E* 72 041903:1-5, 2005.

Ben-Yishai R, Bar-Or RL, Sompolinsky H. Theory of orientation tuning in visual cortex. *Proc Natl Acad Sci* 92(9):3844-8, 1995.

Benda J and Herz AVM. A Universal Model for Spike-Frequency Adaptation. *Neural Computation* 15:2523-2564, 2003.

Brunel N and Hakim V. Fast global oscillations in networks of integrate-and-fire neurons with low firing rates. *Neural Computation* 11(7):1621–1671, 1999.

Buzsáki G. *Rhythms of the brain*. New York: Oxford University Press, 2006.

Celikel T, Szostak VA, Feldman DE. Modulation of spike timing by sensory deprivation during induction of cortical map plasticity. *Nature Neuroscience* 7(5):534-541, 2004.

Davis GW. Homeostatic Control of Neural Activity: From Phenomenology to Molecular Design. *Annual Reviews Neuroscience* 29:307-323, 2006.

Dayan P and Abbott LF. *Theorethical Neuroscience*. Cambridge: MIT Press, 2001.

Destexhe A, Rudolph M, Paré D. The high-conductance state of neocortical neurons *in vivo*. *Nature Reviews Neuroscience* 4:739-751, 2003.

Douglas R and Martin KAC. Neuronal circuits of the neocortex. *Annual Reviews Neuroscience* 27:419–51, 2004.

Dupont E, Canu MH, Falempin M. A 14-Day Period of Hindpaw Sensory Deprivation Enhances the Responsiveness of Rat Cortical Neurons. *Neuroscience* 121:433-439, 2003.

Durstewitz D and Seamans JK. Beyond bistability: biophysics and temporal dynamics of working memory. *Neuroscience* 139(1):119-133, 2006.

Erchova I, Kreck G, Heinemann U, Herz AVM. Dynamics of rat entorhinal cortex layer II and III cells: characteristics of membrane potential resonance at rest predict oscillation properties near threshold. *Journal of Physiology* 560:89-110, 2004.

Evarts EV. Temporal patterns of discharge of pyramidal tract neurons during sleep and waking in the monkey. *Journal of Neurophysiology* 27:152–171, 1964.

Fellous JM, Houweling AR, Modi RH, Rao RPN, Tiesinga PHE, Sejnowski TJ. Frequency dependence of spike timing reliability in cortical pyramidal cells and interneurons. *Journal of Neurophysiology* 85:1782–1787, 2001.

Frazor AR, Albrecht DG, Geisler WS, Crane AM. Visual Cortex Neurons of Monkeys and Cats: Temporal Dynamics of the Spatial Frequency Response Function. *Journal of Neurophysiology* 91:2607-2627, 2004.

Fries P, Reynolds JH, Rorie AE, Desimone R. Modulation of Oscillatory Neuronal Synchronization by Selective Visual Attention. *Science* 291:1560-1563, 2001.

Gabbiani F and Krapp HG. Spike-frequency adaptation and intrinsic properties of an identified, looming-sensitive neuron. *Journal of Neurophysiology* 96:2951-2962, 2006.

Geisler C, Brunel N, Wang X-J. Contributions of Intrinsic Membrane Dynamics to Fast Network Oscillations With Irregular Neuronal Discharges. *Journal of Neurophysiology* 94:4344-4361, 2005.

Gerstner W and Kistler WM. *Spiking neuron models*. Cambridge: Cambridge University Press, 2002.

Grillner S, Markram H, De Schutter E, Silberberg G, Le Beau FEN. Microcircuits in action - from CPG's to neocortex. *Trends in Neurosciences* 28(10):525-533, 2005.

Gonzalez-Islas C and Wenner P. Spontaneous Network Activity in the Embryonic Spinal Cord Regulates AMPAergic and GABAergic Synaptic Strength. *Neuron* 49:563–575, 2006.

Gur M and Snodderly DM. High Response reliability of Neurons in Primary Visual Cortex (V1) of Alert Trained Monkeys. *Cerebral Cortex* 16:888-895, 2006.

Hansel D and Mato G. Existence and stability of persistent states in large neuronal networks. *Physical Review Letters* 86:4175–78, 2001.

Hodgkin AL and Huxley AF. A quantitative description of membrane current and its application to conduction and excitation in nerve. *Journal of Physiology* 117:500-544, 1952.

Hutcheon B, Miura RM, Puil E. Subthreshold membrane resonance in neocortical neurons. *Journal of Neurophysiology* 76(2):683-697, 1996.

Hutcheon B and Yarom Y. Resonance, oscillation and the intrinsic frequency preference of neurons. *Trends in Neurosciences* 23(5):216-222, 2000.

Izhikevich EM. Neural Excitability, Spiking and Bursting. *International Journal of Bifurcation and Chaos* 10(6):1171-1266, 2000.

Izhikevich EM. Resonance and Selective Communication Via Bursts in Neurons Having Subthreshold Oscillations. *BioSystems* 67:95-102, 2002.

Izhikevich EM. Simple Model of Spiking Neurons. *IEEE Transactions on Neural Networks* 14:1569- 1572, 2003.

Izhikevich EM. Which Model to Use for Cortical Spiking Neurons? *IEEE Transactions on Neural Networks (Special Issue on Temporal Coding)* 15:1063-1070, 2004.

Kumar A, Schrader S, Rotter S, Aertsen A. *Dynamics of random networks of spiking neurons with conductance-based synapses*. Cosyne, 2005.

Lampl I and Yarom Y. Subthreshold oscillations and resonant behavior: two manifestations of the same mechanism. *Neuroscience* 78(2):325-341, 1997.

Latham PE, Richmond BJ, Nelson PG, Nirenberg S. Intrinsic Dynamics in Neuronal Networks. I. Theory. *Journal of Neurophysiology* 83:808-827, 2000.

Leung LS and Yu HW. Theta-frequency resonance in hippocampal CA1 neurons in vitro demonstrated by sinusoidal current injection. *Journal of Neurophysiology* 79: 1592–1596, 1998.

Maass W, Natschläger T, Markram H. Real-time computing without stable states: A new framework for neural computation based on perturbations. *Neural Computation* 14(11):2531-2560, 2002.

Miyashita Y and Chang EK. Neuronal correlate of pictorial short-term memory in the primate temporal cortex. *Nature* 331:68–70, 1988.

Mureşan RC and Ignat I. *The "Neocortex" Neural Simulator. A Modern Design*. Proceedings of the International Conference on Intelligent Engineering Systems, September 19-21, Cluj-Napoca, 2004.

Mureşan RC, Pipa G, Florian RV, Wheeler DW. Coherence, Memory and Conditioning. A Modern Viewpoint. *Neural Information Processing - Letters and Reviews* 7(2):19-28, 2005.

Paré D, Lebel E, Lang EJ. Differential Impact on Miniature Synaptic Potentials on the Soma and Dendrites of Pyramidal Neurons In Vivo. *Journal of Neurophysiology* 78:1735-1739, 1997.

Paré D, Shink E, Gaudreau H, Destexhe A, Lang EJ. Impact of Spontaneous Synaptic Activity on the Resting Properties of Cat Neocortical Pyramidal Neurons In Vivo. *Journal of Neurophysiology* 79:1450-1460, 1998.

Pike FG, Goddard RS, Suckling JM, Ganter P, Kasthuri N, Paulsen O. Distinct frequency preferences of different types of rat hippocampal neurons in response to oscillatory input currents. *Journal of Physiology* 29: 205–213, 2000.

Plesser HE and Gerstner W. Noise in Integrate-and-Fire Neurons: From Stochastic Input to Escape Rates. *Neural Computation* 12(2):367-384, 2000.

Puil E, Gimbarzevski B, Miura RM. Quantification of Membrane Properties of Trigeminal Root Ganglion Neurons in Guinea Pigs. *Journal of Neurophysiology* 55(5):995-1016, 1986.

Puil E, Meiri H, Yarom Y. Resonant Behavior and Frequency Preferences of Thalamic Neurons. *Journal of Neurophysiology* 71(2):575-582, 1994.

Richardson MJE, Brunel N, Hakim V. From Sub-threshold to Firing Rate Resonance. *Journal of Neurophysiology* 89:2538-2554, 2003.

Roxin A, Riecke H, Solla SA. Self-Sustained Activity in a Small-World Network of Excitable Neurons. *Physical Review Letters* 92(19):198101, 2004.

Rudolph M, Destexhe A. Event-based simulation strategy for conductance-based synaptic interactions and plasticity. *Neurocomputing* 69:1130-1133, 2006.

Schreiber S, Erchova I, Heinemann U, Herz AVM. Subthreshold Resonance Explains the Frequency-Dependent Integration of Periodic as Well as Random Stimuli in the Entorhinal Cortex. *Journal of Neurophysiology* 92:408-415, 2004.

Sherrington CS. *Integrative Action of the Nervous System*. Yale University Press, 1906.

Softky WR and Koch C. The highly irregular firing of cortical cells is inconsistent with temporal integration of random EPSPs. *Journal of Neuroscience* 13:334-350, 1993.

Steriade M, Nuñez A, Amzica F. Intracellular analysis of relations between the slow (< 1 Hz) neocortical oscillation and other sleep rhythms of the electroencephalogram. *Journal of Neuroscience* 13:3266-3283, 1993.

Steriade M. Grouping of brain rhythms in corticothalamic systems. *Neuroscience* 137(4):1087-1106, 2006.

Timofeev I, Grenier F, Bazhenov M, Sejnowski TJ, Steriade M. Origin of Slow Cortical Oscillations in Deafferented Cortical Slabs. *Cerebral Cortex* 10:1185-1199, 2000.

Torborg CL, Feller MB. Spontaneous patterned retinal activity and the refinement of retinal projections. *Prog Neurobiolog* 74(6):213-235, 2005.

Tsodyks M, Kenet T, Grinvald A, Arieli A. Linking Spontaneous Activity of Single Cortical Neurons and the Underlying Functional Architecture. *Science* 286:1946-1946, 1999.

Tuckwell HC. Stochastic processes in the neurosciences, Philadelphia: SIAM, 1989.

Turrigiano GG and Nelson SB. Homeostatic plasticity in the developing nervous system. *Nature Reviews Neuroscience* 5:97-107, 2004.

Turrigiano GG. Maintaining Your Youthful Spontaneity: Microcircuit Homeostasis in the Embryonic Spinal Cord. *Neuron* 49:481-485, 2006.

Ulrich D. Dendritic Resonance in Rat Neocortical Pyramidal Cells. *Journal of Neurophysiology* 87:2753-2759, 2002.

Vogels TP, Rajan K, Abbott LF. Neural Network Dynamics. *Annual Reviews Neuroscience* 28:357-376, 2005.

van Vreeswijk C and Sompolinsky H. Chaos in neuronal networks with balanced excitatory and inhibitory activity. *Science* 274:1724–1726, 1996.

Wang X. Persistent Neural Activity: Experiments and Theory. *Cerebral Cortex* 13:1123, Special Issue, Persistent Neural Activity: Experiments and Theory, 2003.

Zhang W and Linden DJ. The other side of the engram: Experience-driven changes in neuronal intrinsic excitability. *Nature Reviews Neuroscience* 4:885-900, 2003.

FIGURE LEGENDS:

FIG. 1. Frequency response characteristics of IF, RS and RES neurons to subthreshold input. The neurons are stimulated using a ZAP function (see text for details) and the deviation from rest of their membrane potentials are monitored. The frequency spectra of the membrane potential responses are divided by the frequency spectrum of the input current to yield the frequency-dependent impedances.

FIG. 2. Structure of input spike trains used to assess the suprathreshold frequency response of model neurons. For each frequency of interest (5 to 100 Hz), a Poisson spike train with that mean frequency is produced. The spike trains have different lengths Ws (right) to insure, on average, roughly the same number of input spikes received by the model neurons for all frequencies. The spike trains are only partially plotted (dots).

FIG. 3. Response properties of model neurons to Poisson input spike trains. The total number of spikes (Ψ) in response to various input frequencies and synaptic amplitudes is plotted on the left side. The input spike trains have the structure reported in FIG. 2. On the right, the responses were normalized to the length of the stimulation window (W_s), yielding the firing rate response (R) of the model neurons (see text for details). The ranges of the synaptic amplitude for different models are considered according to a calibration procedure presented in section *Excitability*.

FIG. 4. Effect of an afferent spike arriving at $t=10$ *ms* on different neural models. While the IF and RES models are quite excitable, having large PSP amplitudes, the RS model is responding with much smaller amplitudes. Note that although the synaptic amplitudes (A_{syn}) for excitatory and inhibitory synapses are equal, the actual amplitudes of the two currents are different due to

the difference in driving force of excitatory (reversal potential 0 mV) and inhibitory (reversal potential -90 mV) synapses at rest (see Eq. 5).

FIG. 5. Ratios between the PSP peak amplitudes for different models, as a function of synaptic amplitude *(A_{syn})*.

FIG. 6. Activity patterns in three microcircuits with identical architecture but different excitatory neuron models: IF, RS and RES (spikes of 100 neurons shown for each). After a stimulation phase lasting 50 ms (leftmost spikes, before vertical marker line), the circuits evolve freely (RES) or under the influence of random background currents (IF and RS). The activity patterns look quite different: RES exhibits high frequency oscillations; RS produces some lower frequency oscillations, rather irregularly; IF displays very irregular activity with some inhibited phases around 400 and 800 ms. The after-stimulation response looks quite different in the three cases (50-150 ms on the left of the spike raster, following the 50 ms vertical marker). Examples of typical autocorrelograms computed on the spike trains of the microcircuits are shown on the right (computed for stationary *spontaneous* dynamics, not normalized).

FIG. 7. Self-sustainability of 2000 triplets of networks (with IF, RS and RES excitatory neurons), as a function of synaptic amplitude. The networks are stimulated for 20 ms with a 30 Hz Poisson input and then allowed to evolve freely for 200 ms. Mean and standard deviation of the self-sustained duration of the activity is presented in **a**. In **b**, the percentage of networks that display "explosive" behavior is plotted as a function of synaptic amplitude. The RES synaptic amplitude is taken as a reference, while the amplitudes for the IF and RS networks are rescaled according to FIG. 5.

FIG. 8. Dynamics of "explosive" behavior for IF and RS networks. The population rate is recorded 10 ms before and after the "explosion" of the network activity was detected. The threshold for the detection of "explosive" dynamics (300 Hz) is indicated by arrows. **a.** Population rate dynamics for IF and RS networks, averaged over all synaptic coupling values and all networks that exhibited "explosive" activity. The slope of the rate increase is higher for the IF case. **b.** Population rate dynamics of IF networks with "explosive" activity, for different reference synaptic amplitudes (see text for details). **c.** Population rate dynamics of RS networks with "explosive" activity, for different reference synaptic amplitudes.

FIG. 9. Excitability of different networks to Poisson input of 20 Hz (only the first 200 ms are shown out of the total 1500 ms of the trial). **a.** Population rates are measured for IF, RS and RES networks and averaged over 100 trials and 50 network triplets (see text for details). The most responsive network is clearly IF, followed by RS which displays in addition a clear inhibitory dip after the initial response. RES networks are the least responsive to external input. **b.** Average membrane potential of excitatory neurons in IF, RS and RES networks.

FIG. 10. Population ISI randomness (S_{ISI}) and ISI distributions for three different types of networks. **a.** The average S_{ISI} over 100 trials and 50 networks of each type, as a function of time relative to the beginning of the trial (the first 500 ms of the trial are shown). **b.**, **c.** and **d.** ISI distribution for an IF, RS and RES network, respectively, during the spontaneous, stationary phase of a single trial. A network is considered to be stationary when the ISI population randomness stabilizes (the border is specified by a vertical line in a). Note that the ISI population randomness is dimensionless.

FIG. 11. RS network activity under the influence of spontaneous miniature synaptic potentials. For relatively strong coupling (A_{syn}-RS = 0.03) the network engages in frequent, short lasting bursting events (top trace). The network fires with relatively low frequency (zoomed-in, lower trace, population rate) until a burst event occurs (the population rate is smoothed with a window of 50 ms and a burst is considered to occur when the smoothed rate crosses the threshold of 10 Hz). The membrane potentials of network neurons, plotted in the lower part of the figure (three neurons shown) display frequent, low amplitude spontaneous PSPs due to stochastic miniature synaptic potentials (see bottom-left inset). When a network burst occurs, many neurons engage in burst firing patterns (indicated by the arrow in the lower trace).

FIG. 12. Dependence of the RS networks' activity (under the influence of minis), on different parameters (results averaged over 130 random networks, each simulated for 10^5 ms). **a.** The mean firing rates of RS networks depend on the amplitude of mini PSPs (determined by the Δg-max parameter) and quickly grow with the increase in the excitatory coupling within the network. **b.** The mean baseline firing rates (computed by averaging over the population rate, but leaving out the short burst epochs) increase much slower with coupling than the mean rates. **c.** The number of bursts depends on the mini PSP amplitudes and there is a transition from tonic to bursting regimes induced by the coupling in the network. **d.** and **e.** Burst amplitude (computed as the smoothed population rate during the burst) distributions for two different network couplings (A_{syn}-RS = 0.0275 and 0.0300). The number of bursts depends on the mini PSP amplitudes but the mean burst amplitude is relatively constant for the same network coupling. **f.** The mean and standard deviation computed over the means of different burst amplitude distributions (for different mini PSP amplitudes) for the three coupling strengths where bursting occurs (A_{syn}-RS =

0.0250, 0.0275 and *0.0300*). **g.** and **h.** Inter-burst interval (IBI) distributions, normalized as a fraction of the number of bursts for each mini PSP amplitude. **i.** RS networks display three regimes of activity, depending on the network coupling and mini PSP amplitudes: tonic, aperiodic bursting and periodic bursting.

FIG. 13. Synaptic delays improve the stability of IF and RS networks. **a.** Mean and standard deviation of self-sustained duration of IF networks' activity depending on different maximal synaptic delays. There is no significant difference over different delays and the self-sustained time improves very little. **b.** The self-sustained duration of RS networks' activity is significantly increased because of synaptic delays. **c.** and **d.** Percent of explosive IF and RS networks as a function of synaptic coupling and synaptic delays. The propagation delays shift the threshold of explosion towards higher network coupling strengths.

APPENDIX FIG. 1. Computing the population ISI randomness. We consider a window of 150 ms around a particular time step *t*. An example of a typical window, for a population of 3 neurons is given (upper-left spike raster), with 7 spikes per neuron. This yields 6 ISIs for each neuron (upper-right table), giving a total of 18 ISIs for the entire population ($N_{ISI} = 18$). A population ISI histogram is computed in the first step (bottom chart). After applying an algorithm of clustering on the histogram (see text in APPENDIX), 8 independent clusters can be computed. Each such cluster center is denoted by black arrowheads pointing down. ISIs that are clustered together are denoted by bold underlines, below the *x* axis. The final ISI population randomness is the ratio between the number of independent clusters and the total number of ISIs in the window ($S_{ISI}(t) = 0.44$).

Figure 1.

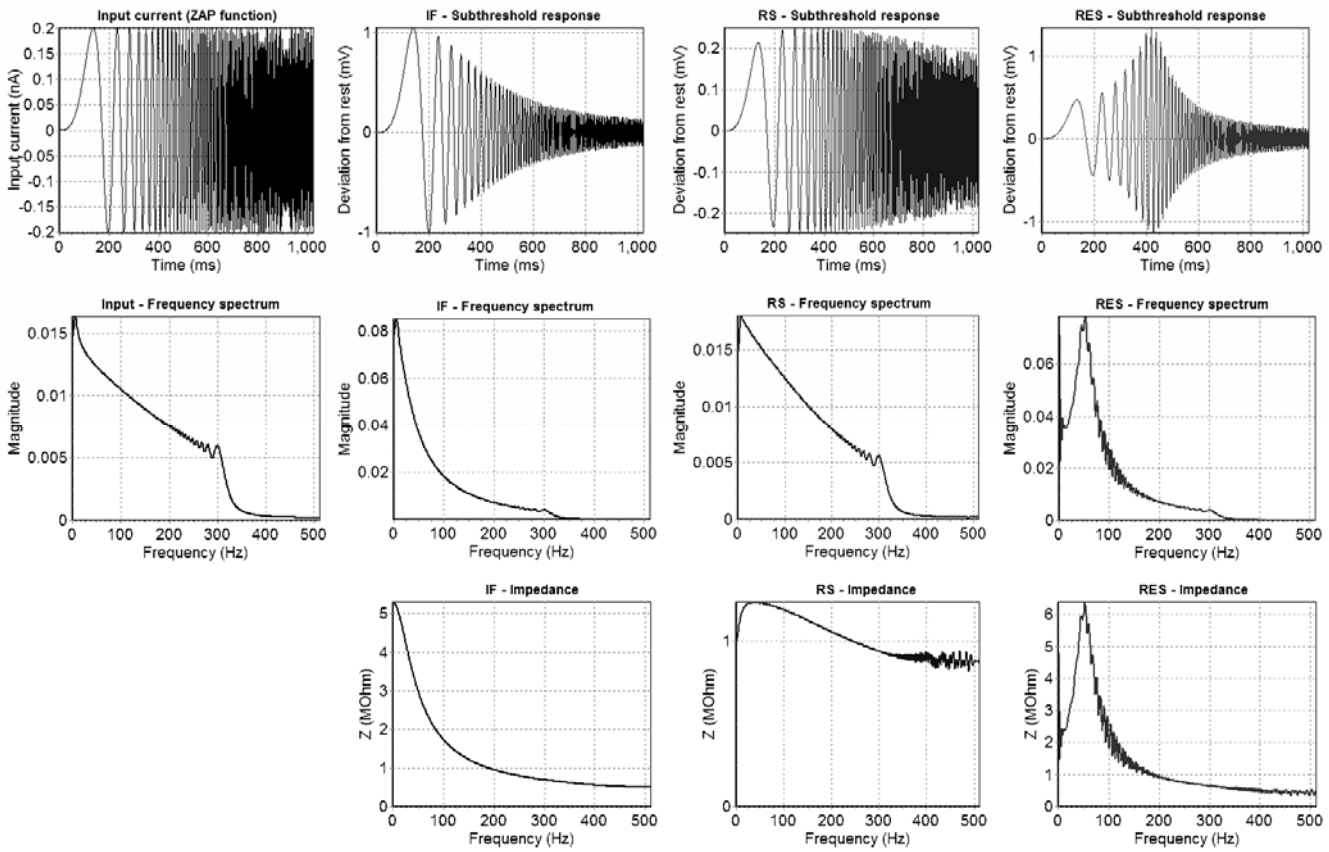
Input current (ZAP function)
Input current (nA)
Time (ms)
IF - Subthreshold response
RS - Subthreshold response
RES - Subthreshold response
Deviation from rest (mV)
Input - Frequency spectrum
IF - Frequency spectrum
RS - Frequency spectrum
RES - Frequency spectrum
Magnitude
Frequency (Hz)
IF - Impedance
RS - Impedance
RES - Impedance
Z (MOhm)

Figure 2.

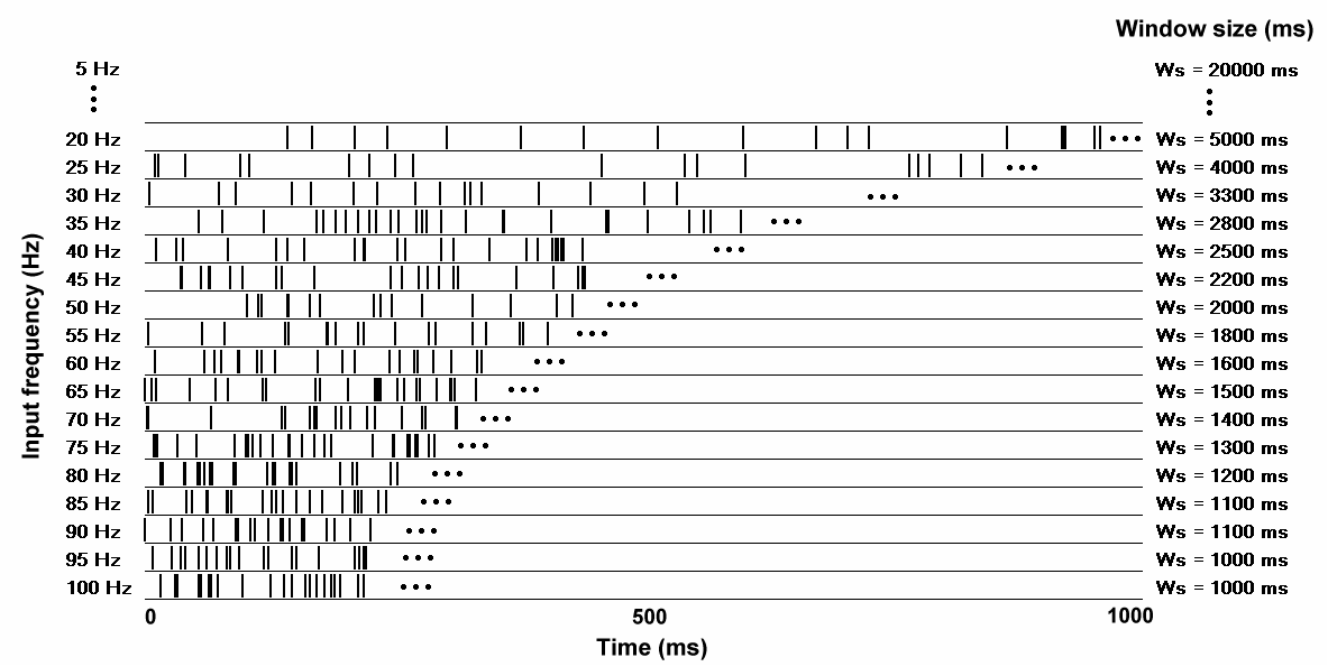
Window size (ms)
5 Hz
20 Hz
25 Hz
30 Hz
35 Hz
40 Hz
45 Hz
50 Hz
55 Hz
60 Hz
65 Hz
70 Hz
75 Hz
80 Hz
85 Hz
90 Hz
95 Hz
100 Hz
Ws = 20000 ms
Ws = 5000 ms
Ws = 4000 ms
Ws = 3300 ms
Ws = 2800 ms
Ws = 2500 ms
Ws = 2200 ms
Ws = 2000 ms
Ws = 1800 ms
Ws = 1600 ms
Ws = 1500 ms
Ws = 1400 ms
Ws = 1300 ms
Ws = 1200 ms
Ws = 1100 ms
Ws = 1100 ms
Ws = 1000 ms
Ws = 1000 ms
Input frequency (Hz)
0
500
1000
Time (ms)

Figure 3.

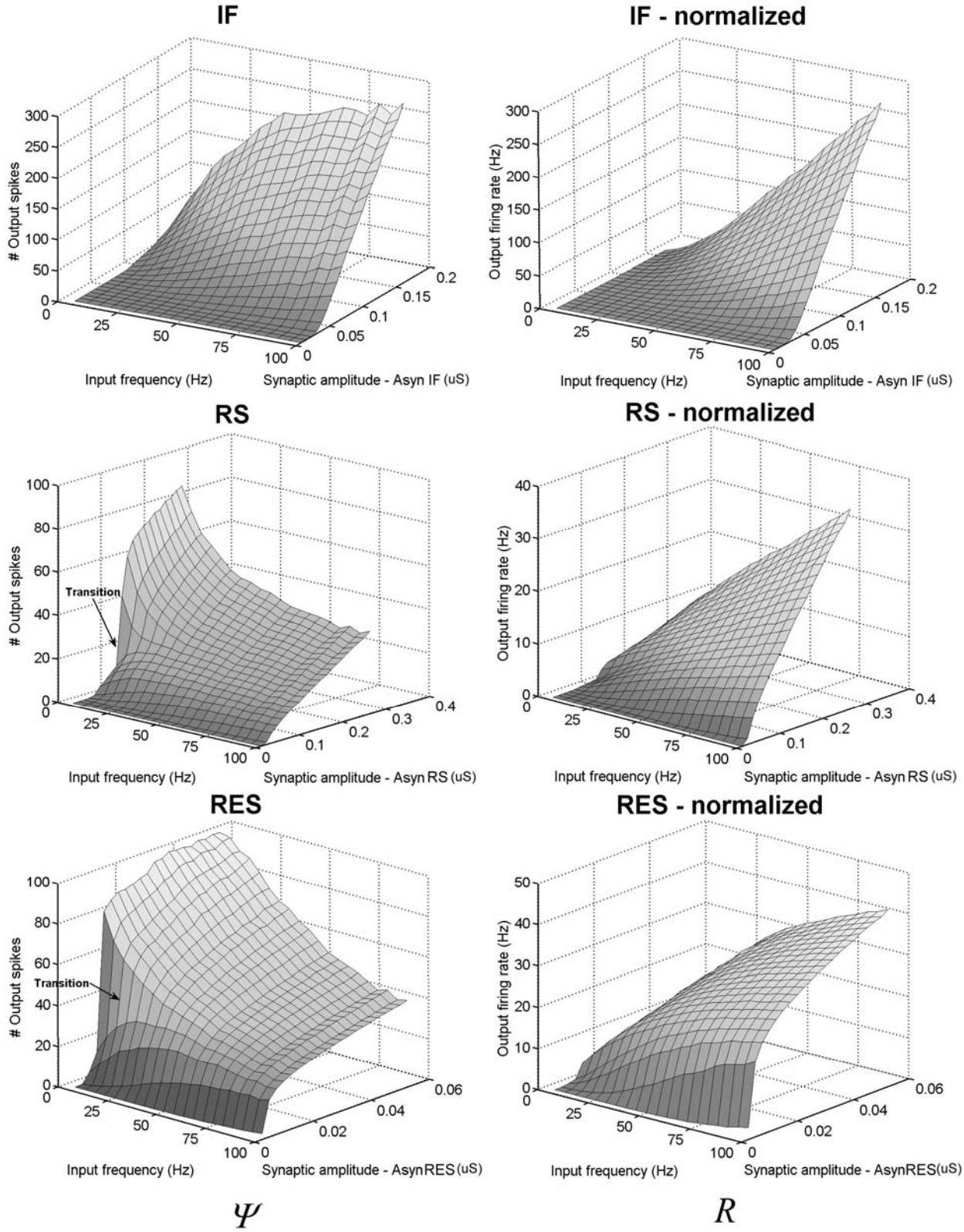

Ψ R

Figure 4.

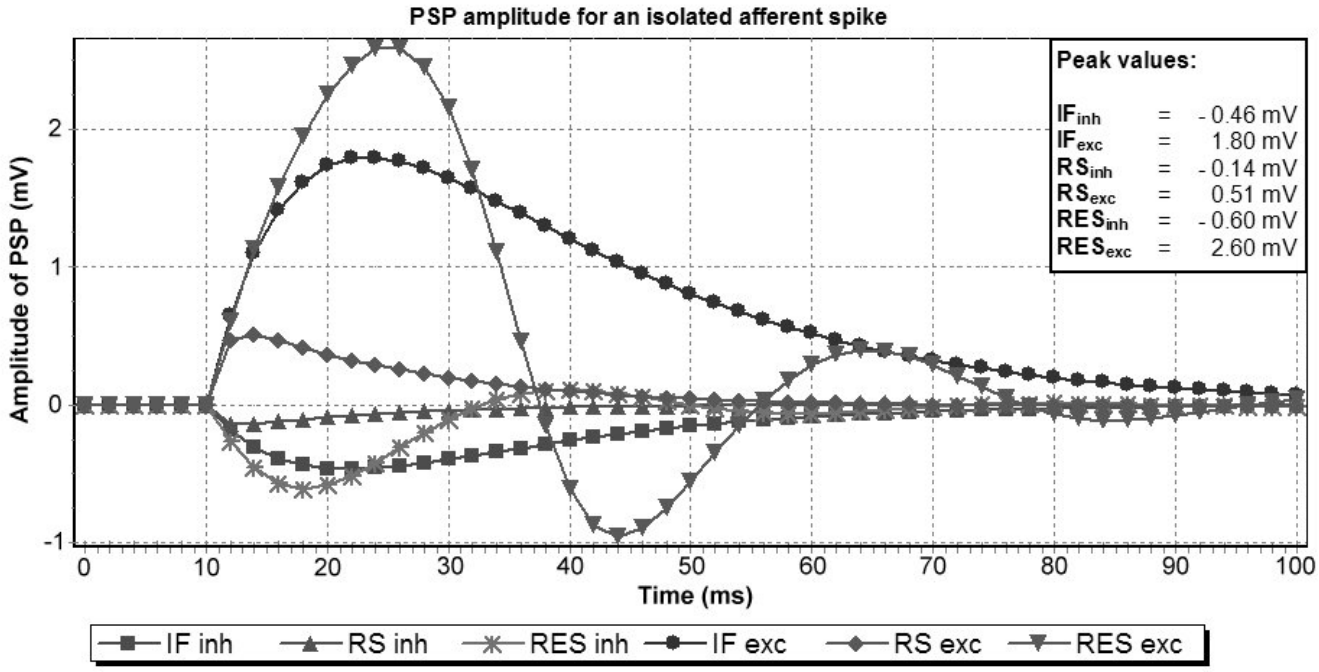
PSP amplitude for an isolated afferent spike
Peak values:
IF inh = - 0.46 mV
IF exc = 1.80 mV
RS inh = - 0.14 mV
RS exc = 0.51 mV
RES inh = - 0.60 mV
RES exc = 2.60 mV
Amplitude of PSP (mV)
Time (ms)
IF inh
RS inh
RES inh
IF exc
RS exc
RES exc

Figure 5.

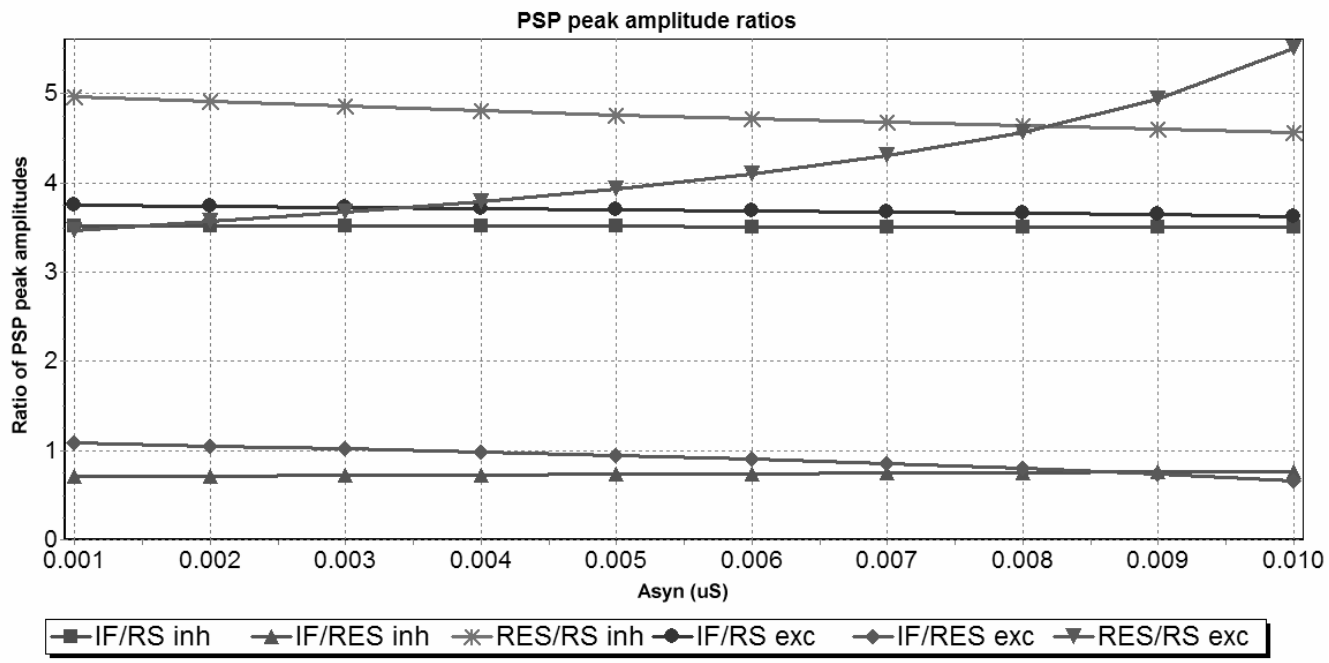
PSP peak amplitude ratios
Ratio of PSP peak amplitudes
0
1
2
3
4
5
0.001
0.002
0.003
0.004
0.005
0.006
0.007
0.008
0.009
0.010
Asyn (uS)
IF/RS inh
IF/RES inh
RES/RS inh
IF/RS exc
IF/RES exc
RES/RS exc

Figure 6.

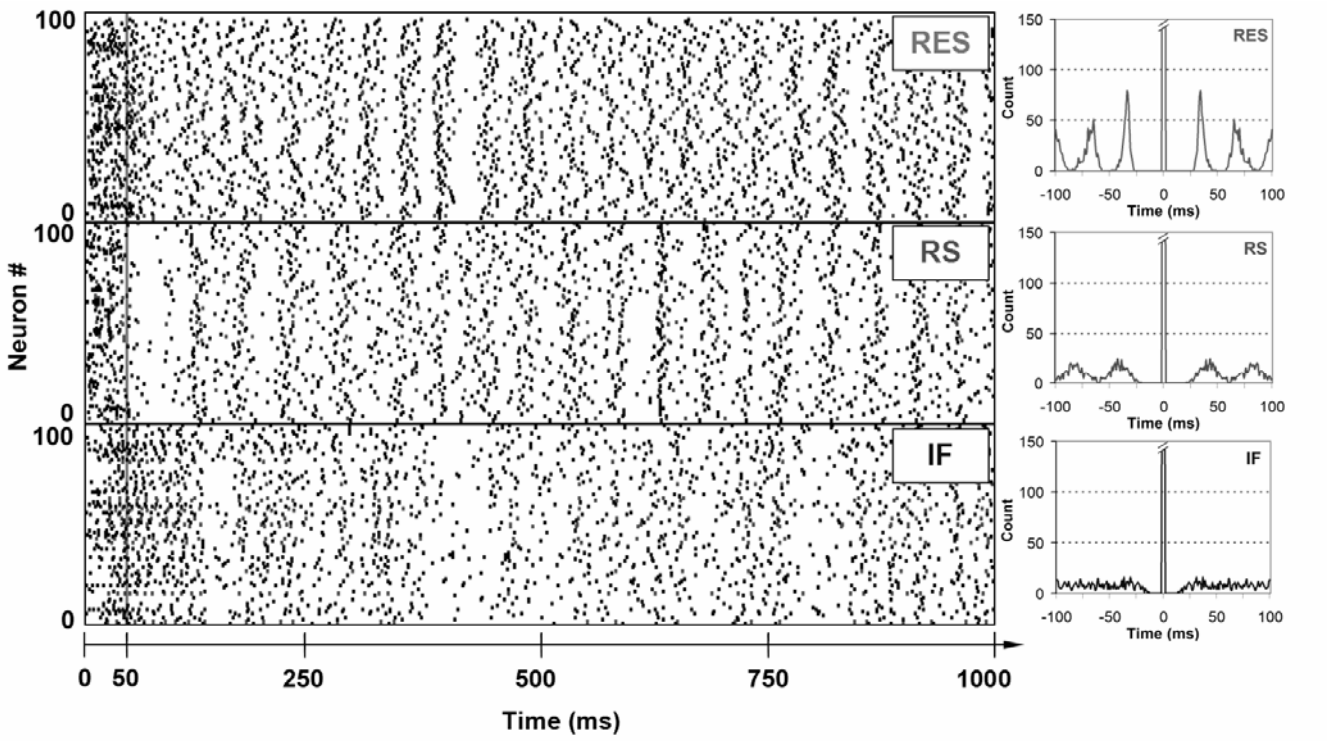
RES
RS
IF
Neuron #
100
0
Time (ms)
0
50
250
500
750
1000
Count
150
-100
-50
50
100

Figure 7.

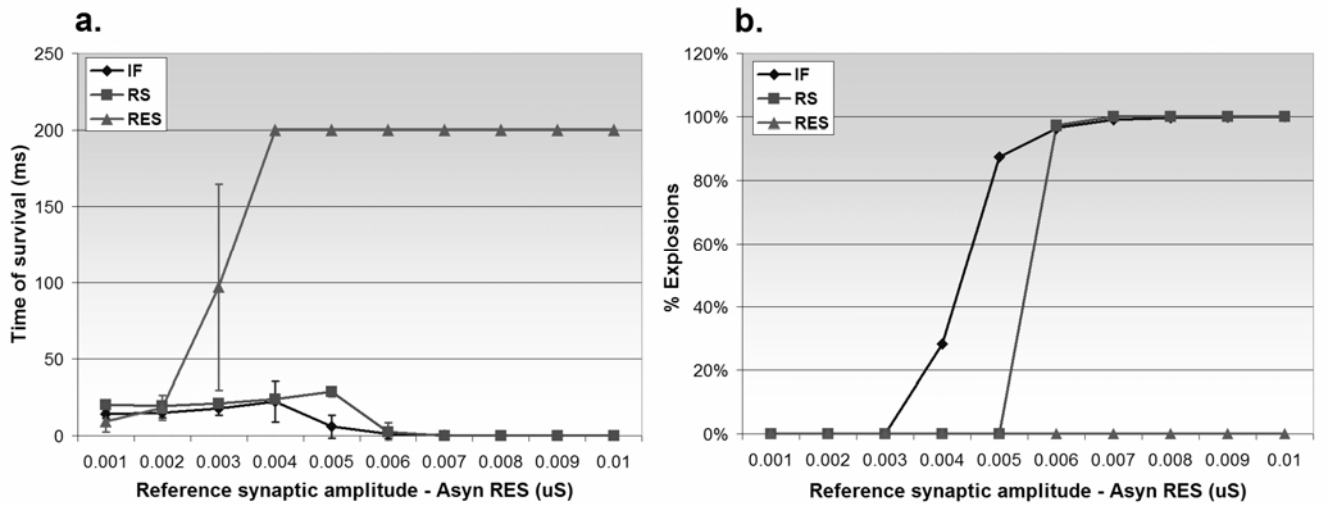
a.
IF
RS
RES
Time of survival (ms)
250
200
150
100
50
0
0.001 0.002 0.003 0.004 0.005 0.006 0.007 0.008 0.009 0.01
Reference synaptic amplitude - Asyn RES (uS)
b.
IF
RS
RES
% Explosions
120%
100%
80%
60%
40%
20%
0%
0.001 0.002 0.003 0.004 0.005 0.006 0.007 0.008 0.009 0.01
Reference synaptic amplitude - Asyn RES (uS)

Figure 8.

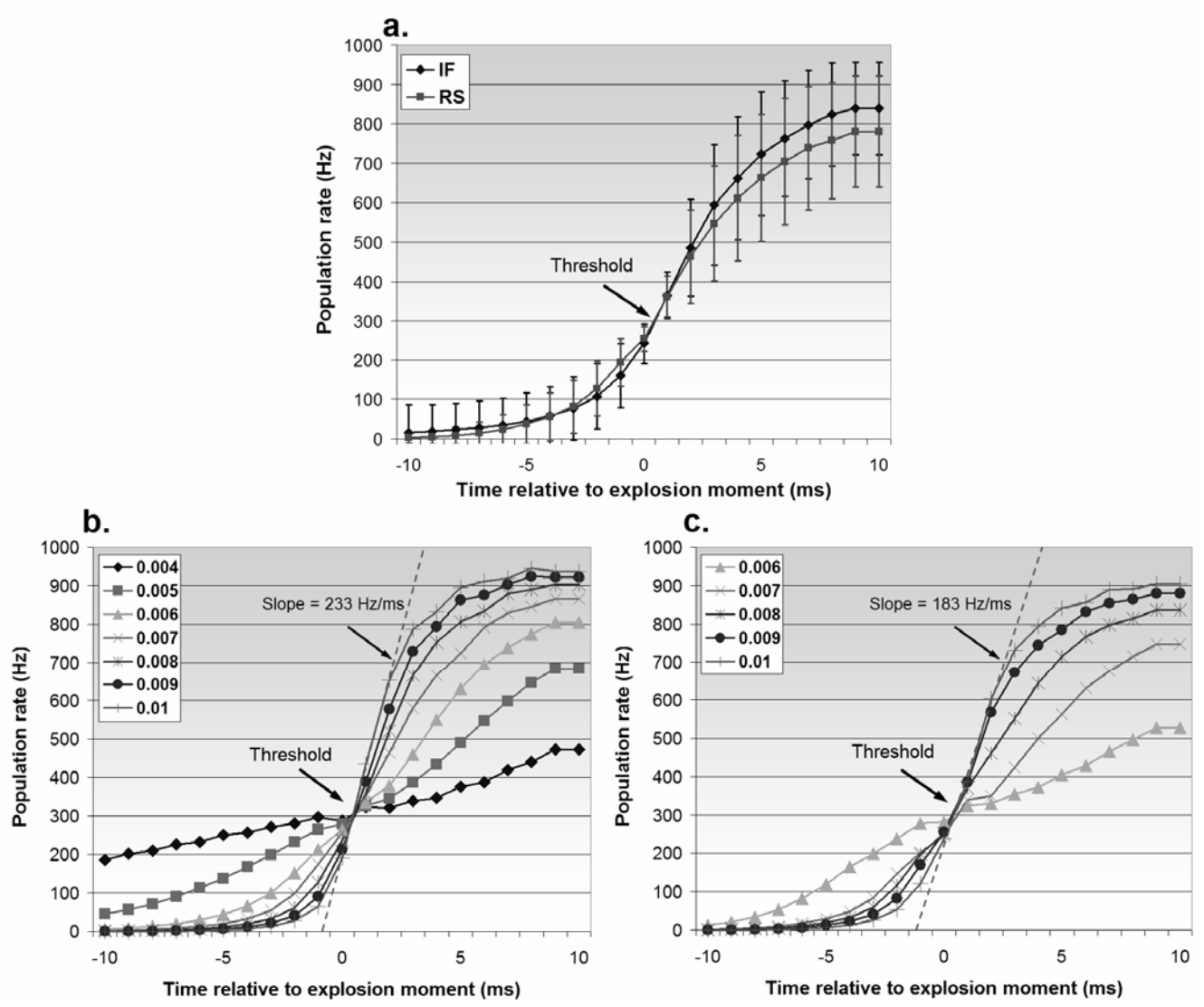
a.
IF
RS
Threshold
Population rate (Hz)
Time relative to explosion moment (ms)
b.
0.004
0.005
0.006
0.007
0.008
0.009
0.01
Slope = 233 Hz/ms
Threshold
Population rate (Hz)
Time relative to explosion moment (ms)
c.
0.006
0.007
0.008
0.009
0.01
Slope = 183 Hz/ms
Threshold
Population rate (Hz)
Time relative to explosion moment (ms)

Figure 9.

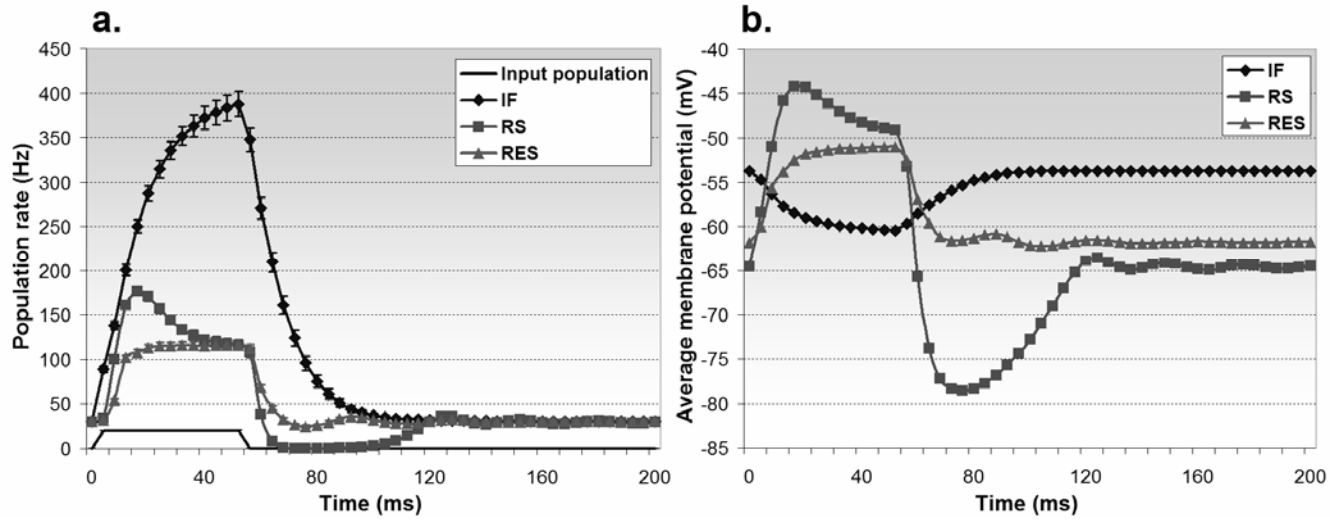
a.
Input population
IF
RS
RES
Population rate (Hz)
Time (ms)
b.
IF
RS
RES
Average membrane potential (mV)
Time (ms)

Figure 10.

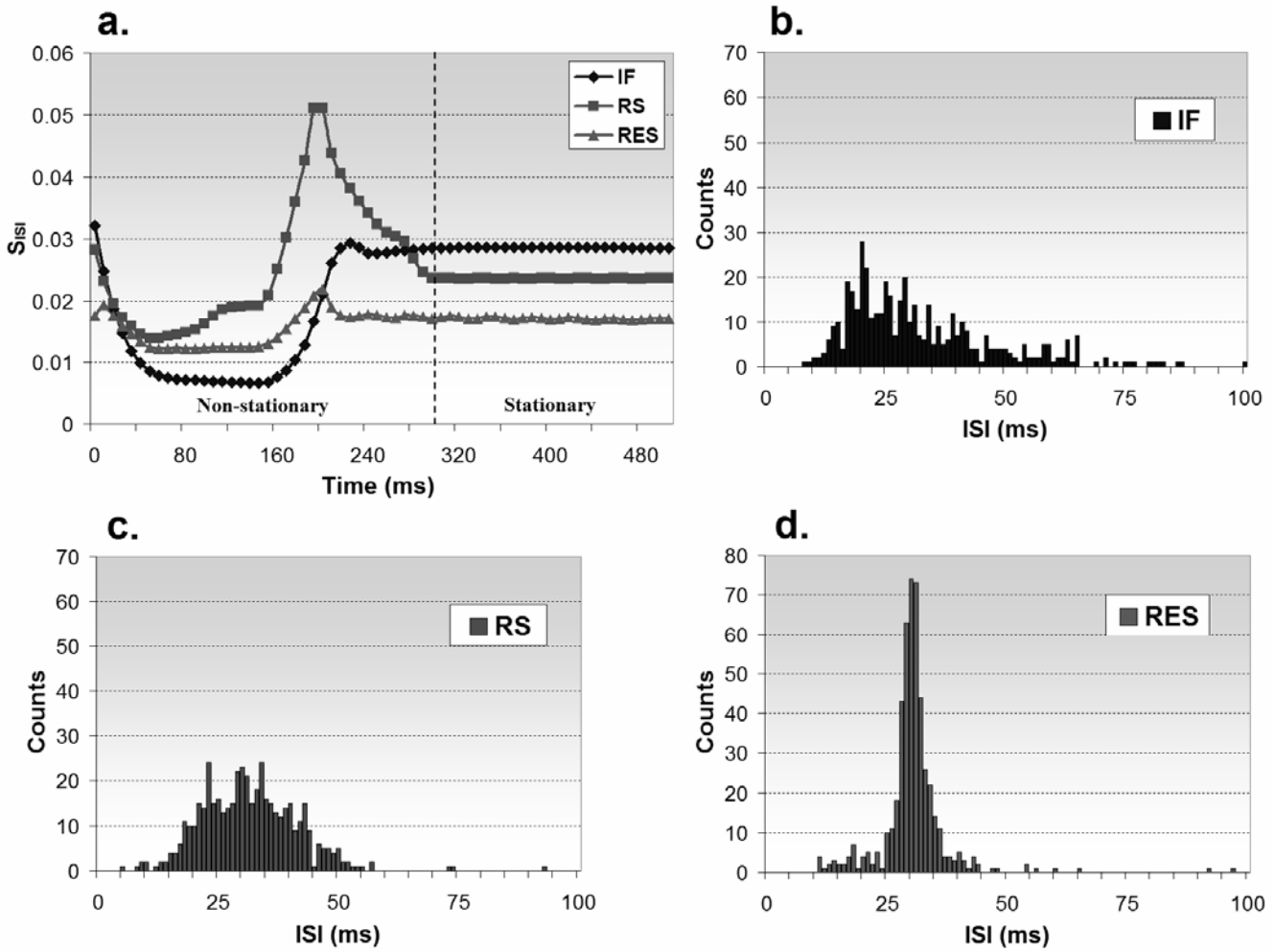
a.
IF
RS
RES
S_{ISI}
Non-stationary
Stationary
Time (ms)
b.
IF
Counts
ISI (ms)
c.
RS
Counts
ISI (ms)
d.
RES
Counts
ISI (ms)

Figure 11.

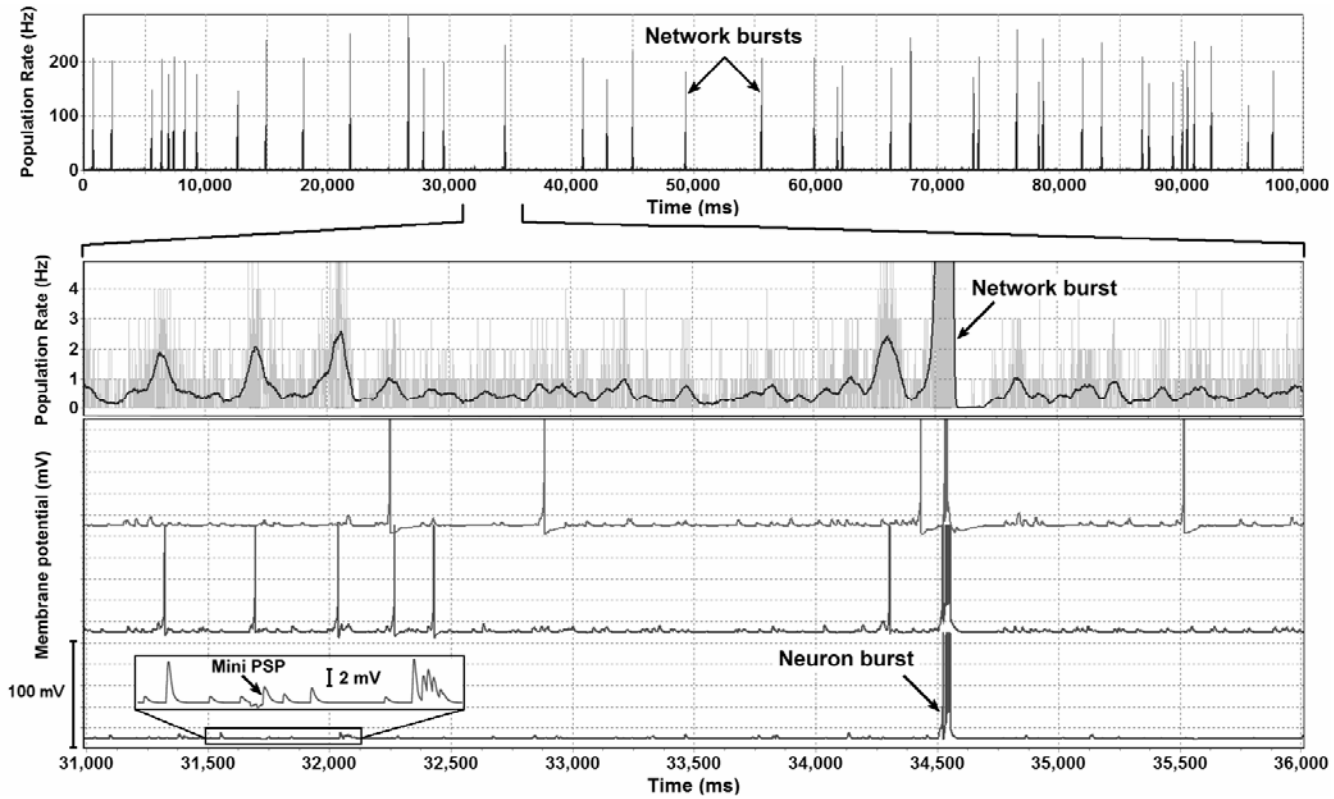
Network bursts
Population Rate (Hz)
Time (ms)
Network burst
Membrane potential (mV)
Mini PSP
2 mV
100 mV
Neuron burst

Figure 12.

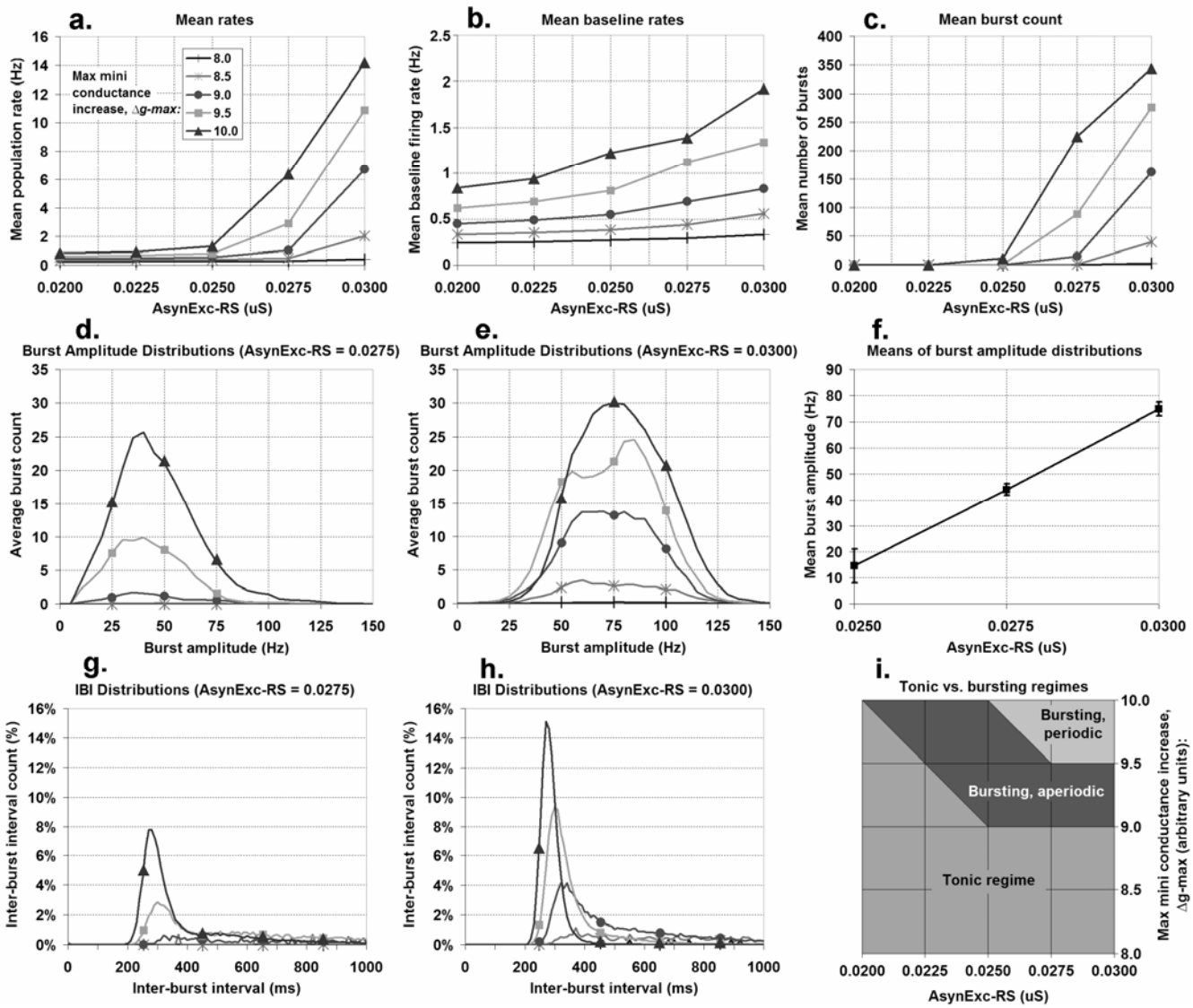
a.
Mean rates
Mean population rate (Hz)
Max mini conductance increase, Δg-max:
8.0
8.5
9.0
9.5
10.0
AsynExc-RS (uS)
b.
Mean baseline rates
Mean baseline firing rate (Hz)
AsynExc-RS (uS)
c.
Mean burst count
Mean number of bursts
AsynExc-RS (uS)
d.
Burst Amplitude Distributions (AsynExc-RS = 0.0275)
Average burst count
Burst amplitude (Hz)
e.
Burst Amplitude Distributions (AsynExc-RS = 0.0300)
Average burst count
Burst amplitude (Hz)
f.
Means of burst amplitude distributions
Mean burst amplitude (Hz)
AsynExc-RS (uS)
g.
IBI Distributions (AsynExc-RS = 0.0275)
Inter-burst interval count (%)
Inter-burst interval (ms)
h.
IBI Distributions (AsynExc-RS = 0.0300)
Inter-burst interval count (%)
Inter-burst interval (ms)
i.
Tonic vs. bursting regimes
Bursting, periodic
Bursting, aperiodic
Tonic regime
Max mini conductance increase, Δg-max (arbitrary units):
AsynExc-RS (uS)

Figure 13.

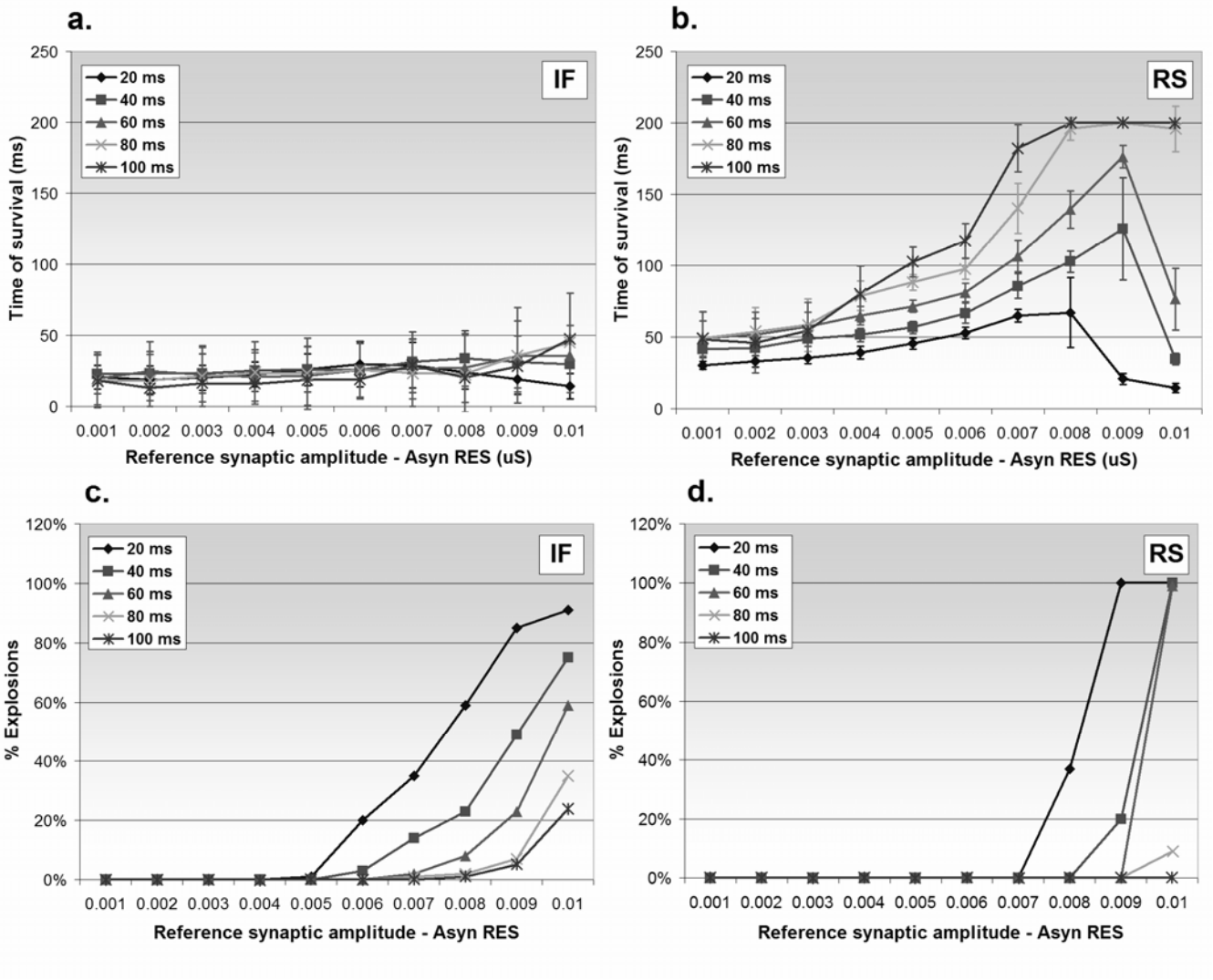
a.
IF
20 ms
40 ms
60 ms
80 ms
100 ms
Time of survival (ms)
Reference synaptic amplitude - Asyn RES (uS)
b.
RS
c.
% Explosions
Reference synaptic amplitude - Asyn RES
d.

Appendix Figure 1.